There is more than one way to force a pendulum

IJMEST

International Journal of Mathematical Education in Science and Technology

ISSN: (Print) (Online) Journal homepage: https://www.tandfonline.com/loi/tmes20

There is more than one way to force a pendulum

Peter Cumber

To cite this article: Peter Cumber (2023) There is more than one way to force a pendulum, International Journal of Mathematical Education in Science and Technology, 54:4, 579-613, DOI: 10.1080/0020739X.2022.2039971

To link to this article: https://doi.org/10.1080/0020739X.2022.2039971

Published online: 11 Mar 2022.

INTERNATIONAL JOURNAL OF MATHEMATICAL EDUCATION IN SCIENCE AND TECHNOLOGY
2023, VOL. 54, NO. 4, 579–613
https://doi.org/10.1080/0020739X.2022.2039971

Taylor & Francis
Taylor & Francis Group

CLASSROOM NOTE

There is more than one way to force a pendulum

Peter Cumber

School of Engineering and Physical sciences, Heriot-Watt University, Edinburgh, UK

ABSTRACT

The dynamics of a simple pendulum are often presented to undergraduate engineering students in introductory courses in dynamics. It is usually the first dynamic system considered by students that is modelled by a differential equation. This paper presents the standard material given to students. It is fair to say that students are accepting this material, but many do not fully appreciate its importance as a basis for the analysis of other dynamic models. Students also believe that the behaviour of a forced simple pendulum is obvious and is not worthy of a deep analysis. This paper presents many interesting results that are available in the open literature, but is not usually presented to undergraduate students. Some of these are counter-intuitive results such as unstable points becoming stable when forced and deterministic models giving chaotic pendulum trajectories. Many results demonstrate that simple pendulums are very interesting and worthy of analysis. The extension of a forced simple pendulum to an application that all students have experience of a child playing on a swing is presented. Only a limited analysis of the swing models is presented. This leaves some open questions for students and lecturers alike to explore.

ARTICLE HISTORY
Received 8 August 2021

KEYWORDS
Mechanics; inverted pendulums; bifurcation; chaos

1. Introduction

The difficulties of inspiring engineering students to engage with machine dynamics are well known (Berry et al., 1989; Biggoggero & Rovida, 1977; Graham & Peek, 1997; Graham & Rowlands, 2000). Dynamics is one of the four engineering sciences that form the basis of nearly all analysis and design in mechanical engineering. This makes the lack of engagement with dynamics by engineering students a problem that must be solved. There has been much research published to identify some of the issues (Fay, 2002; Graham & Rowlands, 2000; Knight, 2004) and presents strategies to address this problem (Graham & Rowlands, 2000; Cumber, 2015; Cumber, 2016). One of the main difficulties is dynamic models are formulated using mathematics at their basis and weaker engineering students do not have the knowledge and skills to formulate or analyse dynamic models using mathematics as a tool. A separate issue is students often try and formulate dynamic models without the use of a free body diagram and mass acceleration diagram. Without these diagrams, it is near impossible to derive dynamic models apart from the most basic such as a box sliding down

CONTACT Peter Cumber p.s.cumber@hw.ac.uk Heriot-Watt University, School of Engineering and Physical sciences, Edinburgh, UK

a slope. This is a problem that has not been considered previously and is a topic for future research.

There have been different approaches to getting through the mathematics to appreciate the dynamics. One approach has been to implement the models as computer programs and solve the underlying equations numerically (Knight, 2004). The numerical simulations allow a student to explore parameter space; however, for the weaker students this often changes the nature of the issue from a lack of understanding of the mathematics to a weakness in programming. More recently, this has been overcome by implementing the model using a graphical user interface (GUI) to set up problems and interrogate results (Cumber, 2015, 2016). Such is the nature of dynamic models; model behaviour can often be illustrated in the form of animations.

The author has produced several papers where the GUI approach has been implemented to allow a student to explore parameter space for a range of dynamic models such as energy harvesters (Cumber, 2016). More information in the use of a pendulum as an energy harvesting device can be found in Yurchenko & Aleras (2013) and Andreeva et al. (2016). Also using GUIs to allow a weaker student to get beyond the mathematical basis, Cumber (2017, 2021) has shown how interesting and, in some cases, non-intuitive dynamic behaviour is possible. In Cumber (2017), the dynamics of a rotating system, is dominated by a body with a centre of mass located off-axis, an unbalanced system, is investigated. Another approach is to show interesting dynamic behaviour for systems that a student is very familiar with, but might not be aware of what dynamic analysis can do. Cumber (2021) is an example of this where the dynamics of a washing machine is investigated. This paper is one of a series that attempts to show it is possible to surprise student engineers by investigating a dynamic system which the student believe they are very familiar with. The point being is that these models make it possible for a student to make connections between dynamics and mechanical devices that they have experience with.

One of the first dynamic systems that an early year's undergraduate student engineer is presented with is a simple pendulum (Fay, 2002). The pendulum dynamics can be considered using an energy method, where there is a balance between the gravitational potential energy and rotational kinetic energy (Meriam & Kraige, 2007). If the pendulum is being forced, then it is more usual to derive a dynamic model using Newton's second law of motion (Meriam & Kraige, 2007). It is often the first dynamic model a student encounters where the acceleration is not constant requiring the model to be derived as a second-order ordinary differential equation. The simple model is also an introductory model for analysing simple harmonic motion, the basis of many topics in physics. Another area of research is investigations of approximate periodic solutions to the simple pendulum equation (Big-Alabo, 2020;Belendez et al., 2006).

In this article, the dynamics of a simple pendulum forced in a variety of ways is presented. The mathematical basis of the models considered are presented, but the models are implemented as part of a GUI to allow the investigation of model behaviour. The point being is that the dynamic behaviour of a forced simple pendulum is very rich, far more complicated, and interesting than most lecturers who deliver early years undergraduate courses in dynamics show their students.

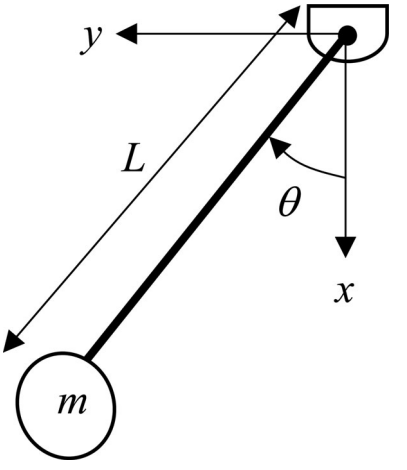

Figure 1. Simple pendulum showing the angular displacement and coordinate axes.

2. Horizontally forced pendulum

In this section, a dynamic model for a forced horizontal pendulum is presented, and the typical dynamic behaviour presented to undergraduate student engineers is discussed.

2.1. Model derivation

We consider the dynamic behaviour of a simple pendulum where the pendulum bob is considered as a point mass at the end of a weightless rod. The pendulum can be excited or forced in several ways. In this section, the pendulum is periodically accelerated horizontally. The coordinate system used is given in Figure 1. The angular displacement, θ is the dependent variable, time, t is the independent variable, m is the mass and L is the length of the rod connecting the bob to the pivot. There are several ways of deriving the equation of motion. The equation of motion without forcing can be derived by applying Newton's second Law of motion in the x and y directions, and then applying the kinematics of the pendulum motion. This approach is a balance between Newton's laws of motion and mathematics. Alternatively, the starting point can be a Lagrangian approach (Meriam & Kraige, 2007). For engineers this is not appropriate, as this generally introduced in an intermediate/advanced level dynamics courses, where multiple degrees of freedom systems are considered. The final method is to take a moment about the pivot and then apply Newton's second law of motion for a rotating system. This is the method of choice as it has the most engineering context. This is important as it is possible to lose the weaker students right at the beginning of the analysis. Sometimes there is too much choice!

The free body diagram and mass acceleration diagram for a horizontally forced pendulum are given in Figure 2. In the figure, T_f denotes the frictional torque at the pivot, T is the tension in the rod connecting the bob to the pivot, I_G is the mass moment of inertia of the pendulum bob about its centre of mass, a_t is the tangential acceleration, a_n is the centripetal acceleration and $\ddot{y}$ is the horizontal acceleration of the pivot. The components of the reaction force at the pivot, O_x and O_y are also shown, although when a moment is

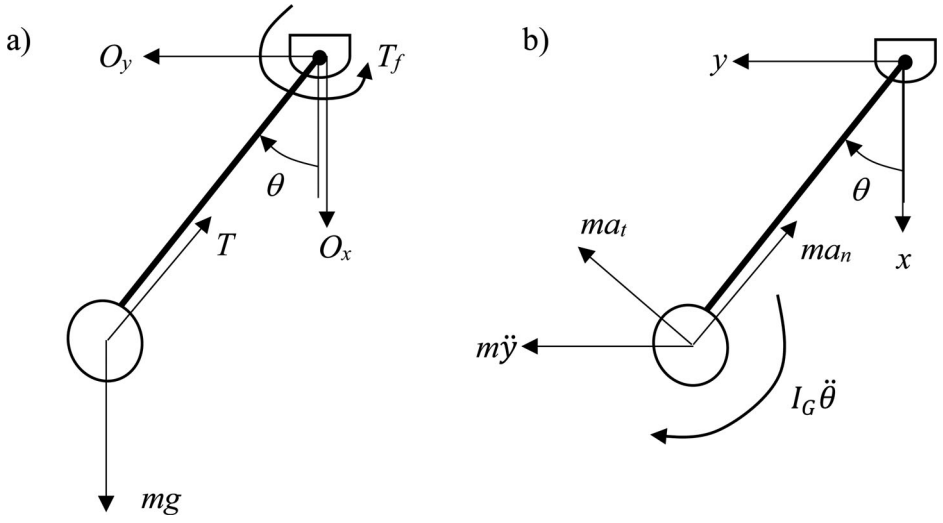

Figure 2. Free body diagram and mass acceleration diagram for a horizontally forced simple pendulum.

taken about O they have no contribution to make to the equation of motion, see below. The free body diagram and mass acceleration diagram represent the equation of motion in a schematic form. The free body diagram represents the left-hand side of (1), and the mass acceleration diagram represents the right-hand side of (1). Taking a moment about the pivot on the left-hand side of (1), we have the moment created by the weight force and the frictional torque, both act in the anticlockwise direction so are defined to be negative. All other forces in the free body diagram have a line of action that passes through the pivot so create no moment. On the right-hand side, we have all of the mass acceleration terms that contribute to the induced moment.

$$-mgL\sin\theta - T_f = I_G\ddot{\theta} + ma_tL + m\ddot{y}L\cos\theta \tag{1}$$

We now simplify the above with the following assumptions and approximations. The bob is modelled as a point mass, the frictional torque, T_f is negligible and specifying the forcing term to be a cosine function of the form

$$y(t) = \mathrm{A}_0\cos\ \Omega\, t \tag{2}$$

Where A_0 is the amplitude of the forcing term and Ω is the forcing frequency. The forcing function (2) together with the relationship between the tangential acceleration and the angular acceleration

$$a_t = L\ddot{\theta} \tag{3}$$

gives

$$L\ddot{\theta} + g\sin\theta = \mathrm{A}_0\Omega^2\cos\theta\cos\Omega t \tag{4}$$

We are now in a position to extend the analysis to look at linear approximations to the pendulum's equation of motion, (4).

2.2. Small amplitude approximation

The pendulum has two steady states, the vertically down position and the vertically up position.

$$\theta = 0 \text{ and } \theta = \pi$$

The vertically down position is stable (or is it!) and the vertically up position is unstable (or is it!). For the vertically down position, it can be useful to use small angle approximations for the sine and cosine function.

$$\sin\theta \approx \theta \; and \; \cos\theta \approx 1$$

Substituting these approximations into (4), gives the pendulum model,

$$L\ddot{\theta} + g\theta = \mathrm{A}_0\Omega^2 \cos\Omega t \tag{5}$$

The small angle approximation gives rise to a linear second-order non-homogeneous differential equation. From this it is possible to derive the natural frequency for the original model, (4).

$$\omega = \sqrt{\frac{g}{L}} \tag{6}$$

A general solution to (5) can be found using standard techniques such as undetermined coefficients and specifying a particular integral based on the functional form of the right-hand side (Glyn & Dyke, 2020). If the natural frequency and forcing frequency are different, then the solution takes the form

$$\theta(t) = c_0 \cos\omega t + c_1 \sin\omega t + \frac{A_0\Omega^2}{L(\omega^2 - \Omega^2)} \cos\Omega t \tag{7}$$

Where c_1 and c_2 are constants fixed by the initial conditions. If the forcing frequency, Ω, is equal to the natural frequency, ω, then the solution is,

$$\theta(t) = c_0 \cos\omega t + c_1 \sin\omega t + \frac{A_0\omega}{2L} t \sin\omega t \tag{8}$$

This is the resonance condition and will be considered in more detail in the next section where the different models, (4) and (5) will be solved numerically.

2.3. Analysis of horizontally forced pendulum

The models (4) and (5) are closed by specifying the initial conditions of the pendulum, θ_0 and $\dot{\theta}_0$. The model can be solved numerically in MATLAB using a numerical ode solver function called **rk45**. The second-order ordinary differential equation (4) must be converted to a first-order system.

$$\begin{pmatrix} \dot{\theta}_1 \\ \dot{\theta}_2 \end{pmatrix} = \begin{pmatrix} \theta_2 \\ \frac{1}{L}(\mathrm{A}_0\Omega^2 \cos\theta_1 \cos\Omega t - g\sin\theta_1) \end{pmatrix} \tag{9}$$

rk45 is an implementation of an ordinary differential equation solver using fourth- and fifth-order Runge–Kutta methods (Lambert, 1991).

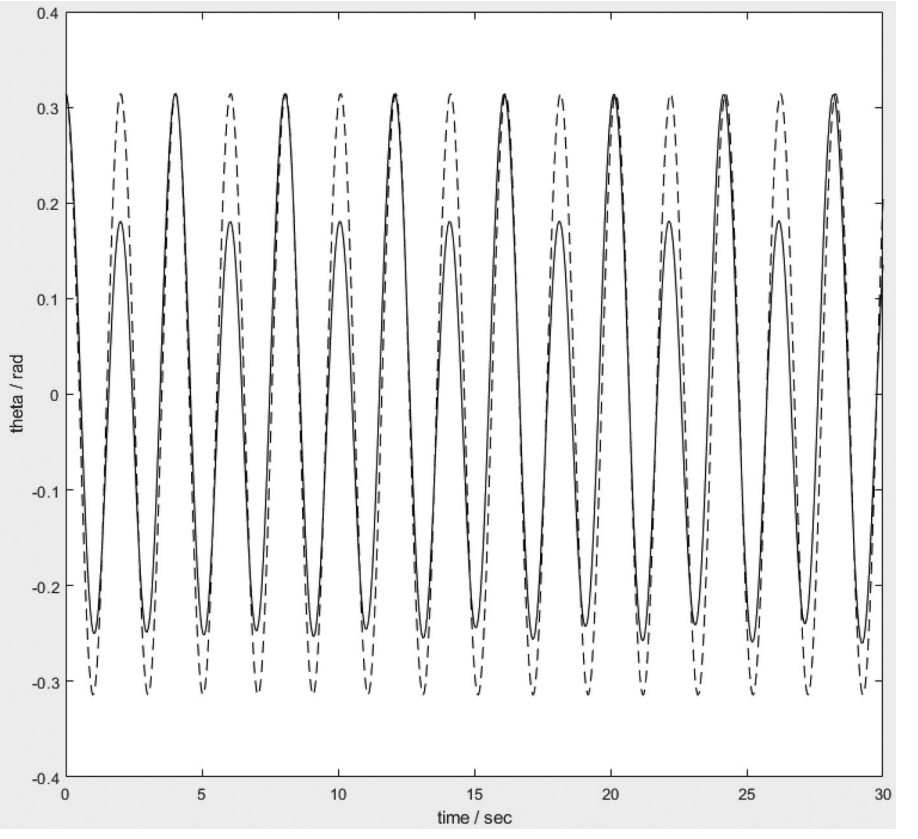

Figure 3. Angular motion of an unforced pendulum and a horizontally forced pendulum, dashed line is unforced, $\theta_0 = \frac{\pi}{10}\text{rad}, \dot{\theta}_0 = 0\frac{\text{rad}}{\text{sec}}, L = 1m$, full line is forced, $A_0 = 0.2m$ and $\Omega = 1.566\frac{1}{s}$.

We can now investigate the dynamic behaviour of the horizontally forced simple pendulum. Two simulations are presented in Figure 3, for each the angular displacement as a function of time is shown. For both simulations, the initial conditions and system parameters are

$$\theta_0 = \frac{\pi}{10}\text{rad}, \dot{\theta}_0 = 0\frac{\text{rad}}{s}, L = 1m$$

In Figure 3, the two simulations differ in the forcing conditions, for the dashed line there is no forcing and for the full line simulation the forcing conditions are,

$$A_0 = \frac{1}{5}L = 0.2m \text{ and } \Omega = \frac{1}{2}\sqrt{\frac{g}{L}} = 1.566\frac{1}{s}$$

These values are chosen to illustrate that the pendulum dynamics are dictated by the natural and forcing frequency. For these simulations, the forcing frequency is half the natural frequency, and we see the pendulum motion to be periodic at the natural frequency with the forcing frequency superimposed on the motion.

We can also use numerical simulation as a tool for exploring how big a range of angular displacement the small angle approximation (5) is valid for. Another interesting thing that

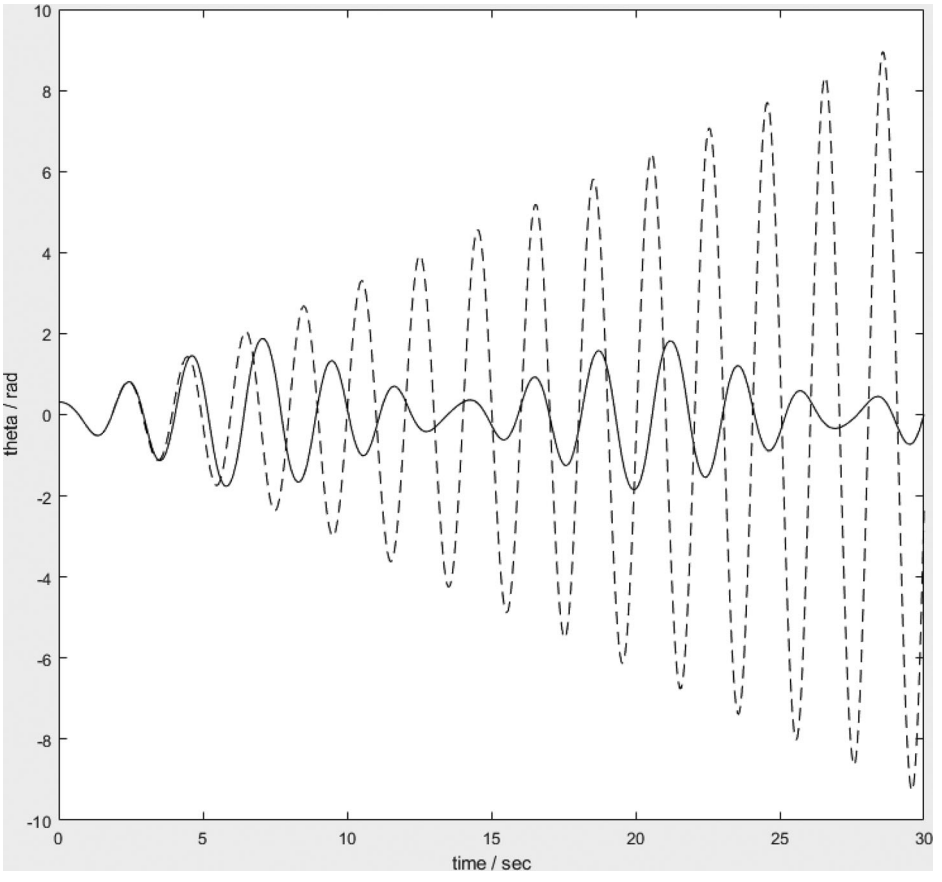

Figure 4. Angular motion of a horizontally forced pendulum, full line is full model, dashed line is the small angle approximation, $\theta_0 = \frac{\pi}{10}\text{rad}, \dot{\theta}_0 = 0\frac{\text{rad}}{\text{sec}}, L = 1m, A_0 = 0.2m$ and $\Omega = 3.132\frac{1}{s}$.

can be done is to force the pendulum at its natural frequency, so-called resonance. Figure 4 illustrates both points. Figure 4 shows the angular displacement for two simulations, the full model and the small angle approximation model, both forced at the natural frequency. The two predictions agree quite well for angular displacements up to $\pi/2$, way beyond the range that the sine and cosine function are well approximated by the small angle approximation. The second feature of note in the figure is the amplitude of the pendulum at the resonance condition for the small angle approximation model is unbounded. This is consistent with the analytical solution, (8), for the linear model, (5). Unfortunately, the small angle approximation does not hold for a time beyond $t = 5$ s.

In dynamics courses, the above is about as much as is typically covered. There might be some discussion of phase space or introduction of energy dissipation due to friction at the pivot and look at over damping, under damping and critical damping but to an undergraduate student engineer, 'We are done with pendulums.'. The above is all very interesting and for someone that has a love of mathematics has a validity that requires no further explanation. To an undergraduate student engineer the question is always how this is going to make me a better engineer. You can justify the analysis of a simple pendulum based on it

will lead on to the analysis of more complex practically based systems. You can certainly demonstrate how resonance is a serious problem in the design of mechanical systems, and students will learn in future dynamics courses how to design to prevent resonance and or for other applications such as energy harvesting, promote resonance (Andreeva et al., 2016; Yurchenko & Aleras, 2013). This is the 'jam tomorrow' justification that the author has not found overly convincing for students in all the years of teaching dynamics or anything else for that matter.

What can we do to help with this situation? One thing that is apparent to someone that teaches pendulum dynamics is that we are selling our subject matter short. There is a wealth of dynamic behaviour exhibited by forced pendulums and much of it is counter-intuitive that is not discussed in the early years undergraduate courses. Apart from resonance most student engineers presented with the above analysis will argue with some justification that they do not know a lot more about pendulums than they did when they started their introductory dynamics course.

3. Vertically forced pendulum

In this section, we will change the direction of forcing to be in the vertical direction and search for counter-intuitive pendulum behaviour.

3.1. Vertically forced pendulum model

The free body diagram for a vertically forced pendulum is the same as a horizontally forced pendulum and is given in Figure 2(a). The mass acceleration diagram for a vertically forced pendulum is shown in Figure 5. Taking these two diagrams and applying the same analysis to derive (1) gives the equation of motion for the vertically forced pendulum as

$$-mgL\sin\theta - T_f = I_G\ddot{\theta} + ma_tL - m\ddot{x}L\sin\theta \tag{10}$$

Assuming the forcing displacement can be given by,

$$x(t) = \mathrm{A}_0\Omega\cos t \tag{11}$$

approximating the pendulum bob as a point mass and neglecting the frictional torque after some simplification gives

$$\ddot{\theta} + \left(\frac{g}{L} + \frac{A_0\Omega^2}{L}\cos\Omega t\right)\sin\theta = 0 \tag{12}$$

If we introduce friction at the pivot then the equation of motion becomes,

$$\ddot{\theta} + \frac{k}{mL}\dot{\theta} + \frac{g}{L}\left(1 + \frac{A_0\Omega^2}{g}\cos\Omega t\right)\sin\theta = 0 \tag{13}$$

Where,

$$T_f = kL\dot{\theta}$$

This is a model for friction that has been used previously (Cumber, 2015). It is common practice to make the above model dimensionless based on the natural frequency. Rather

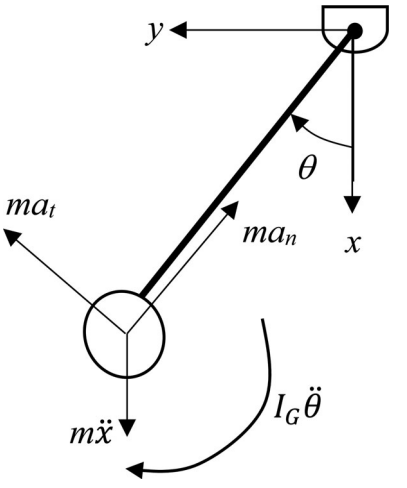

Figure 5. Mass acceleration diagram for a vertically forced simple pendulum.

than do that we will introduce the useful parameters that come out of such a process and specify simulations based on these parameters. The dimensionless form of (13) is often used rather than (13) as it reduces the number of parameters to be considered and the dimensionless parameters left in the model represent the key physics of the dynamic model. For an engineer, the original model is often easier to work with as each parameter has a physical meaning and the independent variable is the real time rather than the scaled time.

The parameters of interest in the analysis below are the frequency factor, ω_0 the amplitude factor, Λ and dimensionless friction coefficient.

$$\omega_0 = \frac{\Omega}{\omega} \tag{14}$$

$$\Lambda = \frac{A_0\Omega^2}{g} \tag{15}$$

and

$$\kappa = \frac{k}{mL\omega} \tag{16}$$

These are dimensionless parameters that measure the forcing frequency compared to the natural frequency, the amplitude of the forcing term and the effects of frictional torque on energy dissipation.

3.2. Stable vs. unstable steady states

Changing the direction of forcing and introducing dissipation introduces some interesting phenomena. For example, when there is no forcing the steady state, $\theta = 0$ rad, is stable. When forcing is introduced depending on the balance between energy dissipation and forcing the steady state, $\theta = 0$ rad, remains stable or becomes unstable as a bifurcation occurs, changing to a stable periodic orbit. Figure 6 shows the angular displacement vs. time and

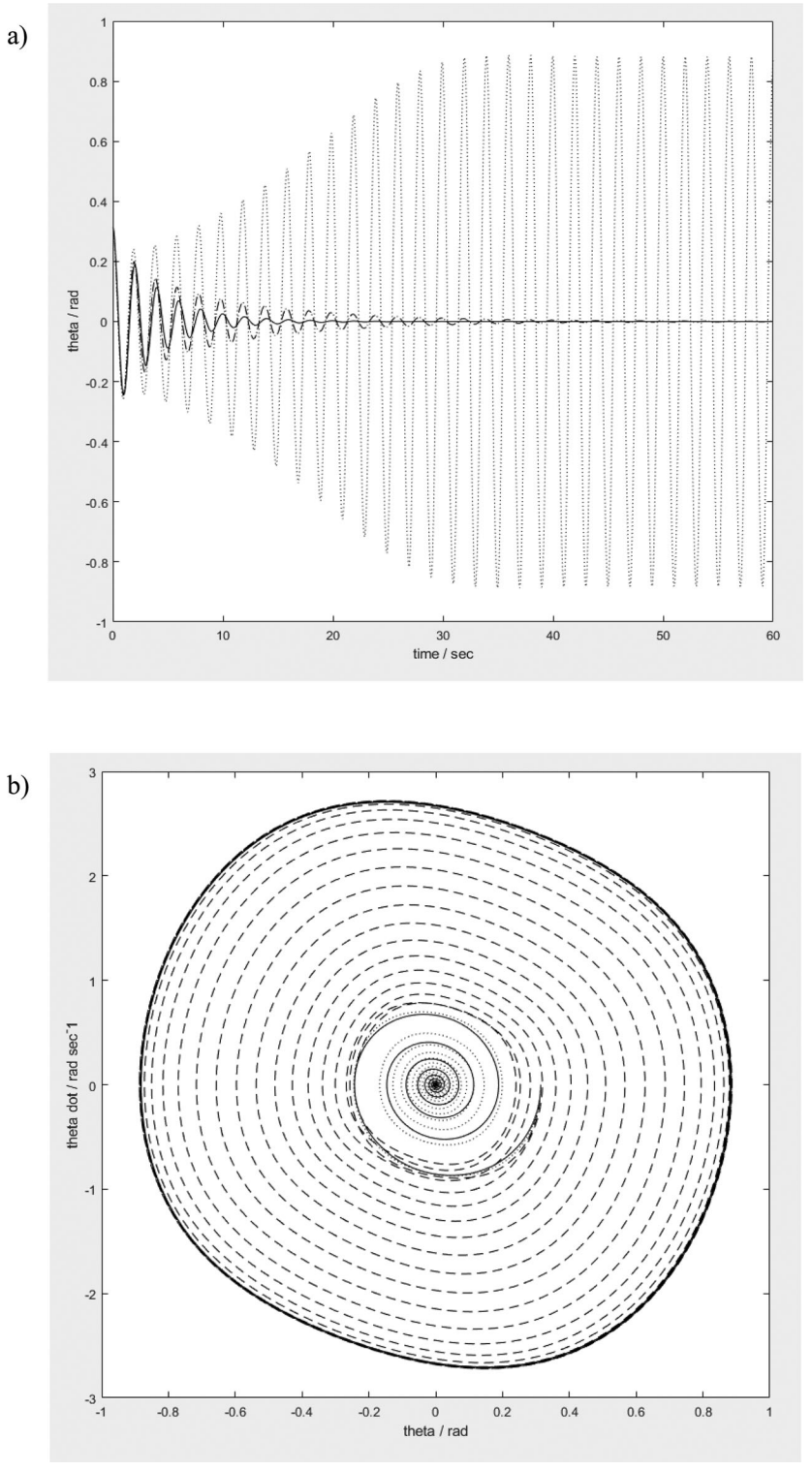

Figure 6. A vertically forced pendulum, $\omega_0 = 2$, full line – $\Lambda = 0.04$, dotted line, $\Lambda = 0.2$, dashed line, $\Lambda = 0.4$, (a) angular displacement vs. time and (b) phase space.

the phase space for three simulations. For all three simulations, the initial conditions and the following parameters are fixed:

$$\theta_0 = \frac{\pi}{10}\text{rad}, \dot{\theta}_0 = 0\frac{\text{rad}}{s}, L = 1m, k = 0.5Ns, \omega_0 = 2$$

The amplitude factor for the three simulations are as follows, full line, $\Lambda = 0.04$, dotted line, $\Lambda = 0.2$ and the dashed line, $\Lambda = 0.4$. For the two smaller amplitude factors, the solution trajectory tends towards the origin, the stable steady state. For the larger amplitude factor, a periodic orbit is clear. This behaviour is even clearer when considering the trajectory in phase space. If you force a pendulum in any other direction, the transition from stable to unstable steady state is not present, forcing changes the stability no matter how big the amplitude or the forcing frequency.

We have a stable point becoming unstable when forcing is introduced. What about the other steady state, $\theta = \pi$? Can forcing make an unstable steady-state stable? The answer is yes. Consider the simulations shown in Figure 7. In Figure 7, again three simulations are shown. This time the initial conditions and other parameter values are

$$\theta_0 = \frac{9\pi}{10}\text{rad}, \dot{\theta}_0 = 0\frac{\text{rad}}{s}, L = 10m, k = 0.5Ns$$

Note that the pendulum length has been increased to 10 m, changing the natural frequency to be approximately unity and the initial pendulum orientation is close to the unstable steady state value, $\theta = \pi$. Using the frequency factor to identify the three simulations in Figure 7, for the lower frequency values, $\omega_0 = 5.05$ and 10.1, the pendulum rapidly moves away from the unstable steady state, $\theta = \pi$ rad and tends to the stable steady state, $\theta = 0$ rad. The pendulum oscillates with decreasing amplitude. After 60 s of simulation time the solution is still periodic. If the simulation were continued, the pendulum trajectory would tend further to the steady state $\theta = 0$ rad. For the high-frequency forcing simulation, $\omega_0 = 20.2$, the pendulum trajectory is very different. The solution remains in the vicinity of a vertically orientated pendulum with the solution tending to the unstable steady state, $\theta = \pi$. After 60 s the solution is quasi-periodic oscillating about the steady state, $\theta = \pi$, with diminishing amplitude. If the simulation were continued, then the pendulum trajectory would tend to the unstable steady state, $\theta = \pi$. This is a well-known result in the pendulum research community but not so with undergraduate engineers. It is possible to demonstrate it to students using a high-speed electric drill or jig saw, (https://www.youtube.com/watch?v=5oGYCxkgnHQ). The first publication on this phenomenon is probably (Stephenson, 1908), and it is investigated experimentally and the explanation for why it happens is given in Kapitza (1965). There have been many more publications on stabilizing an inverted pendulum since then. A more recent publication with a clear explanation for why an inverted pendulum can be stabilized by vertical forcing is given in Butikov (2001). If you integrate the imposed mass acceleration over a single cycle of the pivot motion, the integral is zero. If you consider the integral of the induced moment over a cycle of the pivot under certain circumstances, it is not zero. If the pivot is vertically forced with sufficient frequency and amplitude, then over a cycle of the pivot motion the average moment of the mass acceleration acts to accelerate the pendulum towards the inverted orientation and is larger than the moment produced by the weight, see Butikov (2001).

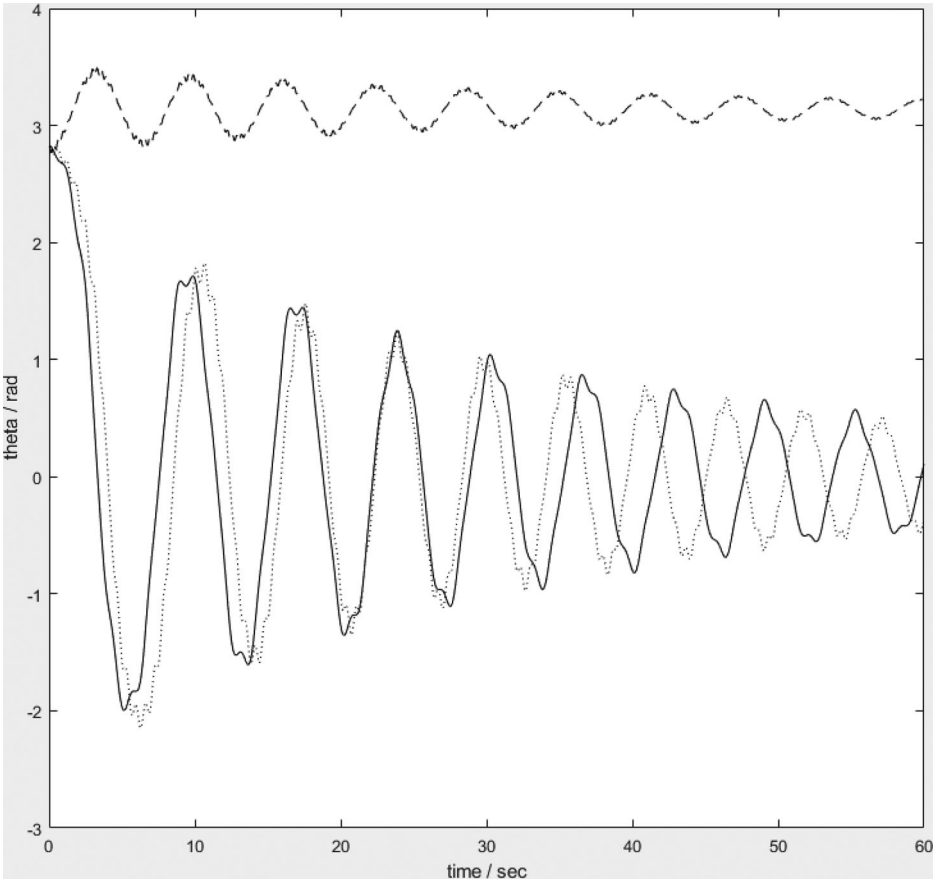

Figure 7. Angular displacement vs. time for a vertically forced pendulum, full line – $(\omega_0, \Lambda) = (5.05, 2.55)$, dotted line $(\omega_0, \Lambda) = (10.1, 10.2)$ and dashed line, $(\omega_0, \Lambda) = (20.2, 40.8)$.

An unstable steady state is made stable by forcing the system. This is an interesting counter-intuitive result. It is a memorable result that students find engaging, demonstrating that there is more to pendulums than they might have originally believed. Maintaining a pendulum at or near its inverted orientation is a classic control engineering problem. Control engineering is an important advanced topic in dynamics usually covered in the later years of an undergraduate degree programme. This gives an important link to future studies in dynamics and demonstrates an interesting idea for maintaining a pendulum in a vertical orientation, rather than use a complicated control system to maintain the pendulum in an unstable state, you could make it stable by forcing the pendulum.

3.3. Basins of attraction

Having demonstrated that the forced pendulum is stable in an inverted orientation for a specific set of initial conditions, an obvious question is for what set of initial conditions and forcing pendulum parameters is the steady state $\theta = \pi$, stable? For a given frequency factor, amplitude factor and friction coefficient the set of initial conditions that tend to the

steady state $\theta = \pi$, is called a basin of attraction and is defined to be the set,

$$B_A = \{(\theta_0, \dot{\theta}_0), \theta(t) \to \pi, as\, t \to \infty\} \tag{17}$$

For the set of forcing conditions and pendulum parameters,

$$m = 1\text{kg}, L = 10m, k = 0.5Ns, \omega_0 = 20.2, \Lambda = 40.8$$

an approximation to the set, B_A is calculated numerically by simulating the pendulum trajectory for a matrix of initial conditions, $(\theta_0, \dot{\theta}_0)$,

$$0 \leq \theta_0 \leq 6\text{rad}$$

$$-2 \leq \dot{\theta}_0 \leq 2\frac{\text{rad}}{s}$$

In Figure 8, discuss below, the matrix of points consists of 400 spanning the range of the domain for the initial angular displacement and angular velocity. A number of numerical experiments were completed to determine appropriate parameter values for determining the basin of attraction. For each set of initial conditions, a simulation is completed with a simulation time of $t_{\max} = 30$ s. The initial conditions are considered a member of the basin of attraction if the inequality

$$|\theta(t_{\max}) - \pi| \leq \frac{\pi}{10}$$

is satisfied. This will produce a subset of B_A but it will give a good indication of the range of initial conditions that will tend towards the unstable steady state, $\theta = \pi$.

Figure 8 shows two basins of attraction for an inverted pendulum, $L = 10$ m, with vertical forcing, $(\omega_0, \Lambda) = (20.2, 40.8)$. Two basins of attraction are shown, with two different values for the friction parameter. In Figure 8(a), $\kappa = 0.0505$ and in Figure 8(b), $\kappa = 0.0101$. Qualitatively the basins of attraction are similar with a region of phase space close to the steady solution being in the basin of attraction. For larger values of θ_0 and $\dot{\theta}_0$, a spiral pattern that is antisymmetric about the line $\theta_0 = 0$ is present in both figures. As the energy dissipation is reduced the size of the basin of attraction reduces. The qualitative shape of the basins of attraction computed in this paper is similar to those presented in Wright et al. (2014).

3.4. Stability regions

Another interesting issue is the determination of the range of frequency factor and amplitude factor that the basin of attraction set for the steady state $\theta = \pi$ is finite, i.e. there is a set of pendulum initial conditions that tend to the steady state.

A subset of the stability region can be generated numerically. The approximate stability region for the steady state $\theta = \pi$ is shown in Figure 9(a). The stability region is calculated by generating a matrix of 400×400 points in frequency factor/amplitude factor space in the region,

$$1 \leq \omega_0 \leq 4$$

$$0 \leq \Lambda \leq 5$$

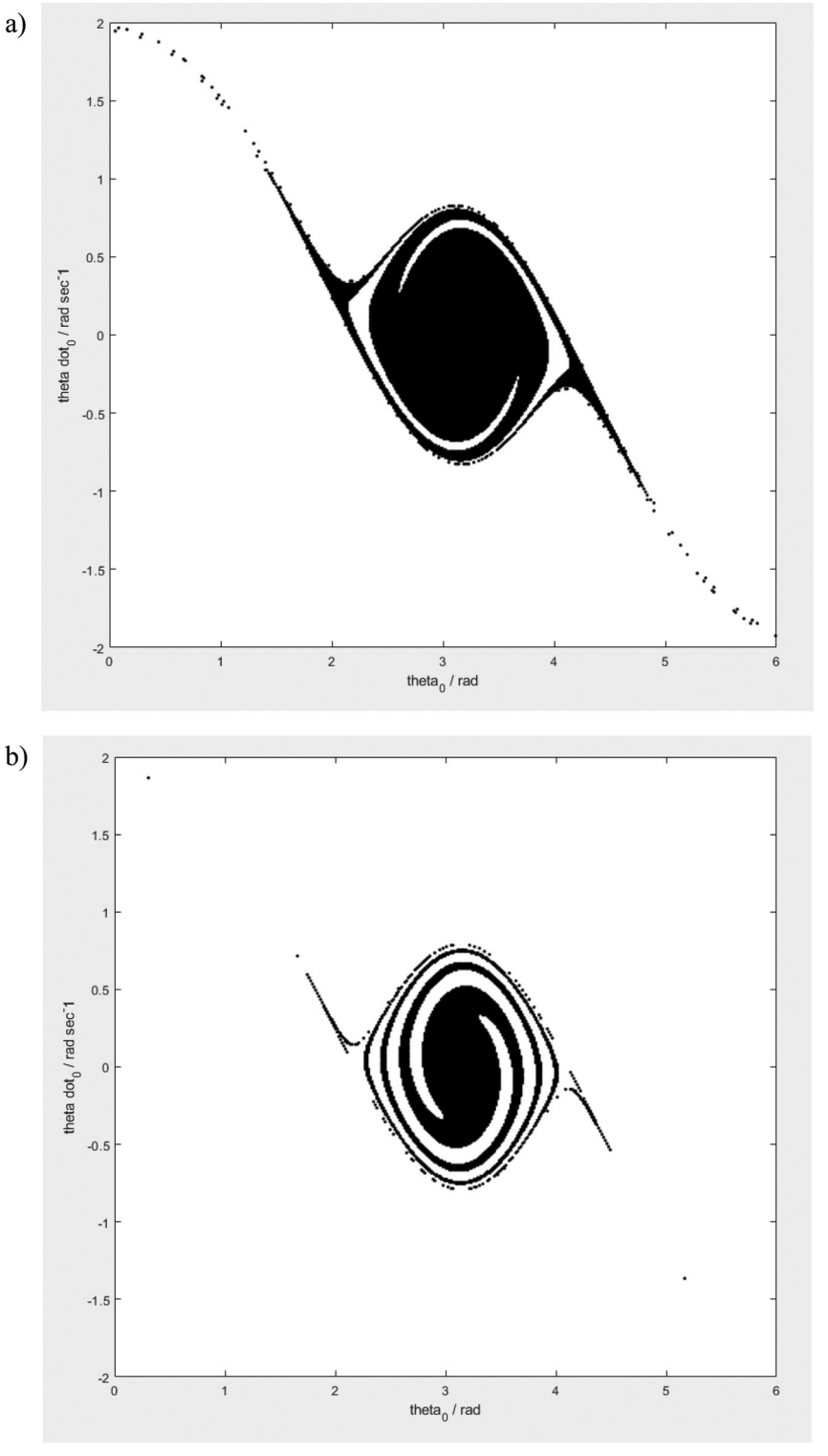

Figure 8. Basins of attraction for a vertically orientated pendulum, $L = 10$ m, $(\omega_0, \Lambda) = (20.2, 40.8)$, (a) $\kappa = 0.0505$ and (b) $\kappa = 0.0101$.

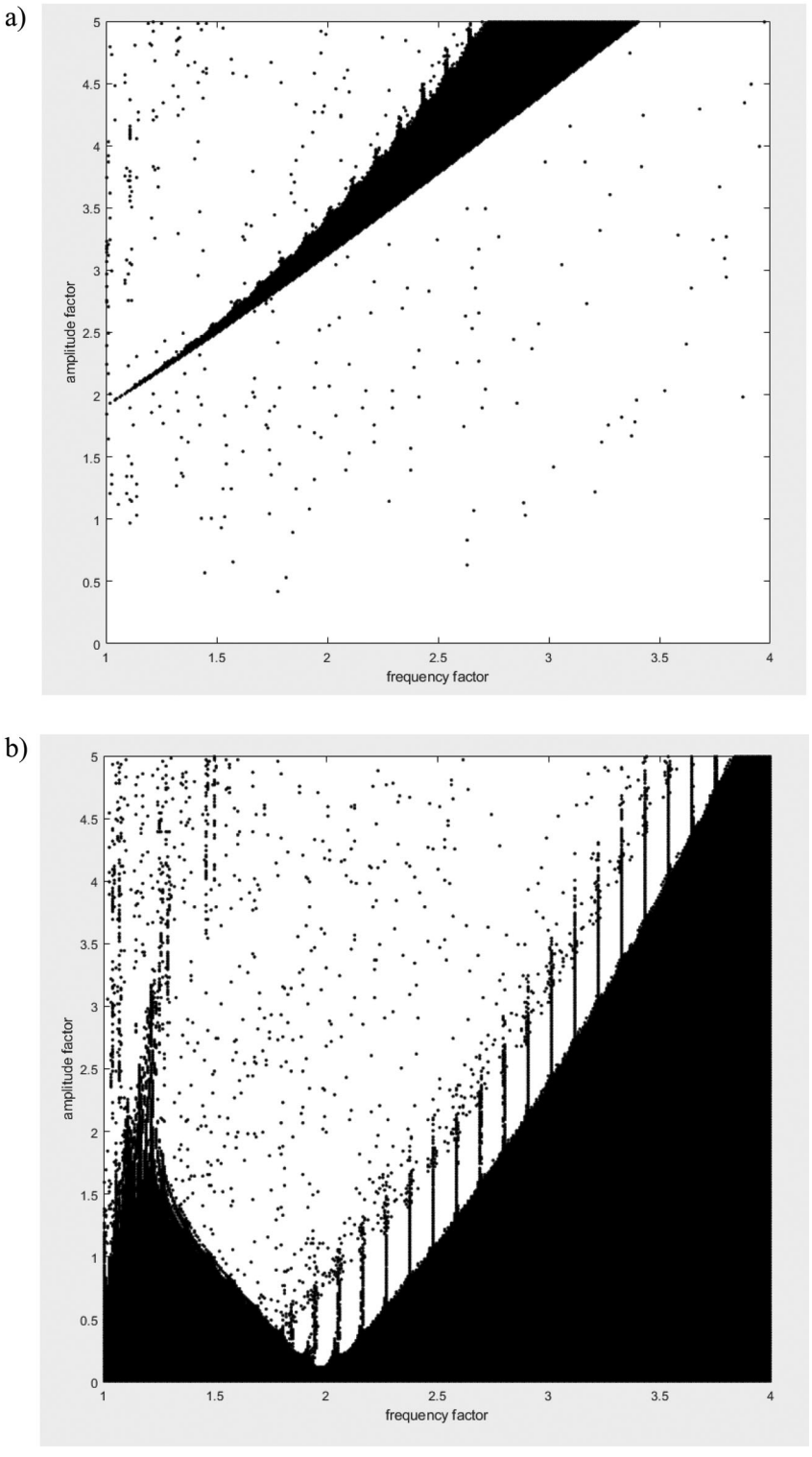

Figure 9. Stability region for the steady state, $\kappa = 0.0505$, (a) $\theta = \pi$, and (b) $\theta = 0$.

For each point in frequency factor/amplitude factor space, the vertically forced pendulum is run for a matrix of initial conditions for a maximum time of $t_{\max}$ seconds. This is a potentially compute intensive process if a lot of starting conditions are considered with a large simulation time; however, if a sparce matrix of initial conditions are considered or $t_{\max}$ is too small, then the stability region will be underestimated. After a preliminary set of numerical experiments, $t_{\max}$ was set at 60 s and a matrix of 5×5 starting conditions in the region of initial condition space given below.

$$\frac{19}{20}\pi \leq \theta_0 \leq \frac{21}{20}\pi \,\text{rad}$$

$$-0.5 \leq \dot{\theta}_0 \leq 0.5\frac{\text{rad}}{s}$$

For the simulations used to calculate the stability region the following pendulum parameters are specified:

$$m = 1kg, L = 10m, k = 0.5Ns$$

A point in frequency factor/amplitude factor space is considered part of the stability region if at least one point of the matrix of 5×5 initial conditions simulations converges to the steady state. The condition used is

$$|\theta(t_{\max}) - \pi| \leq \frac{\pi}{100}$$

Figure 9(a) shows the generated stability region for $\theta = \pi$. There are a number of isolated points that are either part of the stability region or require more simulation time to move away from the steady state, $\theta = \pi$. The transition to a stable steady state in frequency/amplitude parameter space as the amplitude parameter increases from zero is clear in Figure 9(a) and is represented approximately by a line passing through or close to the two points $(\omega_0, \Lambda) = (1, 2)$ and $(\omega_0, \Lambda) = (3.4, 5)$. The shape of the stability region has a cusp initiated at a point near $(\omega_0, \Lambda) = (1, 2)$. On the upper edge of the stability region, the shape has a 'saw-tooth' structure.

A similar stability region for the steady state $\theta = 0$ is shown in Figure 9(b). As one might expect, we see a bigger region of stability. There are some interesting features that require further discussion. The steady-state solution for a frequency factor close to two becomes unstable for relatively small values of the amplitude factor. This is consistent with the stability analysis given in Nayfeh (1993), where the damped Mathieu equation (Nayfeh, 1993), the dimensionless linearized version of (13) demonstrates the existence of 'tongues' of instability centred on, vertical lines in frequency factor/amplitude factor space given by the expression

$$\frac{4}{\omega_0^2} = n^2, n = 1, 2, \ldots \tag{18}$$

In Figure 9(b), the instability region centred on $\omega_0 = 2$ is equivalent to (18) with $n = 1$. Another interesting feature of the stability region are the equi-spaced lines of stability for the frequency factor above two. The spacing is approximately a little under 0.1 in frequency factor. Difficult to appreciate what is going on from a theoretical viewpoint,

but numerical simulation has proved a useful tool for identifying these structures in frequency factor/amplitude factor space. A limited search of the literature has not revealed any publications on this behaviour.

3.5. Bifurcation and chaos

Given the stability regions discussed above do not cover the whole range of frequency factor/amplitude factor space a good question is 'What is the long-term asymptotic state of a vertically forced pendulum where the pendulum does not tend towards a steady state?'. Defining the asymptotic set,

$$\{\theta^* = \theta(t), \text{where } \dot{\theta}(t) = 0, t \to \infty\} \tag{19}$$

for a given, κ, ω_0 and Λ. This is the equivalent of looking at a Poincare map in phase space $(\theta, \dot{\theta})$ by drawing a line, $\dot{\theta} = 0$ (Guckenheimer & Holmes, 2002). This is a useful tool as it reduces the two-dimensional phase space to a single dimension, angular displacement. The numerical implementation of this can be done using linear interpolation. The numerical implementation of the asymptotic set and the Poincare map is as follows. Given the numerical simulation of the pendulum, we have an array of points that are a numerical solution of the differential equation (13).

$$\{(\theta, \dot{\theta})(t_i), i = 1, 2, \ldots, N_{\text{pts}}\} \tag{20}$$

Then points in the asymptotic set are calculated by looking for turning points in the array of points. The following condition is used for a turning point:

$$\dot{\theta}(t_j)\dot{\theta}(t_{j+1}) \leq 0$$

Together with linear interpolation to calculate the asymptotic state as,

$$\theta^* = \frac{\theta_{j+1}\dot{\theta}_j - \theta_j\dot{\theta}_{j+1}}{\dot{\theta}_j - \dot{\theta}_{j+1}} \tag{21}$$

The asymptotic set of angular displacements, θ^* for a pendulum, with the following parameters:

$$m = 1\text{kg}, L = 10m, k = 0.5Ns, \omega_0 = 3.5$$

is shown in Figure 10. The figure is generated by calculating the asymptotic set for a 1000 uniform values of the amplitude factor in the range,

$$0 < \Lambda < 9$$

For each simulation, the simulation time is taken to be 600 s. For each simulation, the last 10% of values are used to calculate the angular displacement at an angular velocity of zero. The simulation time and the proportion of the simulation used to determine the asymptotic set is found by completing a number of numerical experiments to ensure the predictions shown in Figure 10 are a true representation of the asymptotic set.

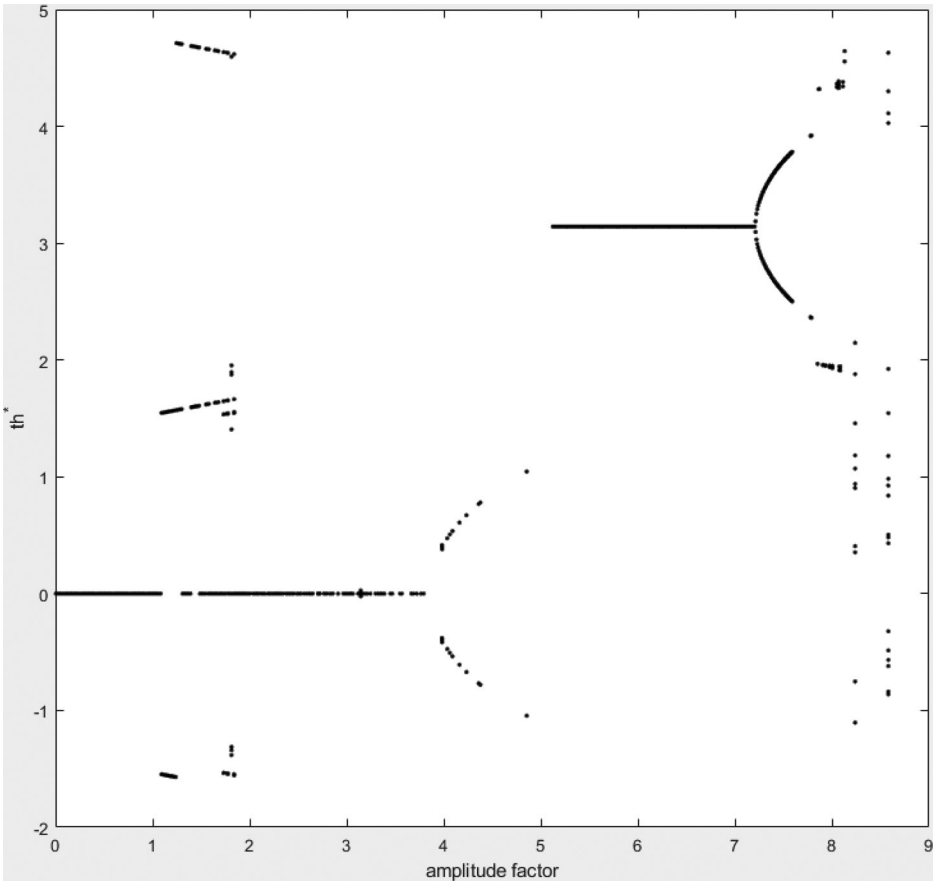

Figure 10. The asymptotic set vs. amplitude factor for $L = 10$ m, $k = 0.5$ N s and $\omega_0 = 3.5$.

For each simulation, the initial condition was specified to be close to the inverted pendulum orientation

$$\theta_0 = \frac{19}{20}\pi \text{rad}, \dot{\theta}_0 = 0\frac{\text{rad}}{s}$$

This is done to capture any pendulum simulations that tend towards the inverted pendulum steady state. A further point of note is that in Figure 10 the angular displacement range is adjusted to be

$$-\frac{\pi}{2} \leq \theta \leq \frac{3\pi}{2}$$

rather than,

$$-\pi \leq \theta \leq \pi$$

This gives a clearer picture of the asymptotic behaviour of the pendulum for this set of pendulum parameters and initial conditions. In Figure 10, for small values of the amplitude factor the asymptotic set consists of the steady state, $\theta = 0$. As the amplitude factor

increases to a value just above one, the asymptotic set for this initial condition is a periodic solution of period 3. This exists for a small interval of amplitude factor space, until the amplitude factor reaches a value of approximately 1.5–1.8, when the asymptotic set again reduces to the vertically down orientation. Increasing the amplitude factor further to a value just below 4 a bifurcation occurs and a periodic solution of period 2 becomes the asymptotic state. Increasing the amplitude factor further to a value of 5 the asymptotic state from this initial condition is a single point once again, but this time it is the inverted pendulum orientation, $\theta = \pi$. Note the oscillating solution centred on $\theta = 0$ could still be stable for higher amplitude factors and given a different initial condition would be recovered as part of the asymptotic set. Returning the focus to the inverted pendulum state, this continues for values of the amplitude factor above 5 to a maximum amplitude value of approximately 7.4. Beyond this point in amplitude factor space, another period doubling bifurcation occurs giving an oscillating solution centred on $\theta = \pi$. Beyond an amplitude factor of approximately 7.6 the oscillating solution is no longer part of the asymptotic set and is replaced with something with a more complex structure. A further point of note is that for some values of the amplitude factor the asymptotic set is null. In this context, a null asymptotic set is indicative of a pendulum undergoing full rotations rather than being stationary or oscillating.

The dynamic behaviour of the pendulum shown in Figure 10 and discussed above is very rich and deserves further investigation. Rather than do that attention will be given to a pendulum that more clearly exhibits the classic period doubling sequence on route to chaotic behaviour (Sander & Yorke, 2012).

The pendulum under investigation in this part of the paper is a vertically forced pendulum, (13) with the following pendulum parameters:

$$m = 1\text{kg}, L = 1m, k = 1Ns, \omega_0 = 2.5$$

For the simulations considered below, the initial condition is

$$\theta_0 = \frac{\pi}{10}\text{rad}, \dot{\theta}_0 = 0\frac{\text{rad}}{s}$$

An initial condition close to the steady state, $\theta = 0$ is imposed as for the forcing conditions given the inverted pendulum is not stable so is not of interest. For these parameter values, the asymptotic set is plotted for a range of the amplitude factor,

$$1.2 < \Lambda < 2.8$$

Figure 11(a) is generated in the same way as Figure 10. The asymptotic behaviour of the pendulum is similar to that shown in Figure 10. For small values of the amplitude factor, the solution tends to the steady state $\theta = 0$. At around an amplitude factor of 1.3, the solution bifurcates to give an oscillating solution with growing amplitude as the amplitude factor increases. At a value of the amplitude factor just above 2.4, the asymptotic set has a different structure, but it exists for only a small interval of the amplitude factor. This will be considered further below. The periodic solution returns as the only member of the asymptotic set until a value of the amplitude factor of approximately 2.6 is reached, and a second period doubling bifurcation occurs to give an oscillating solution with a cycle of

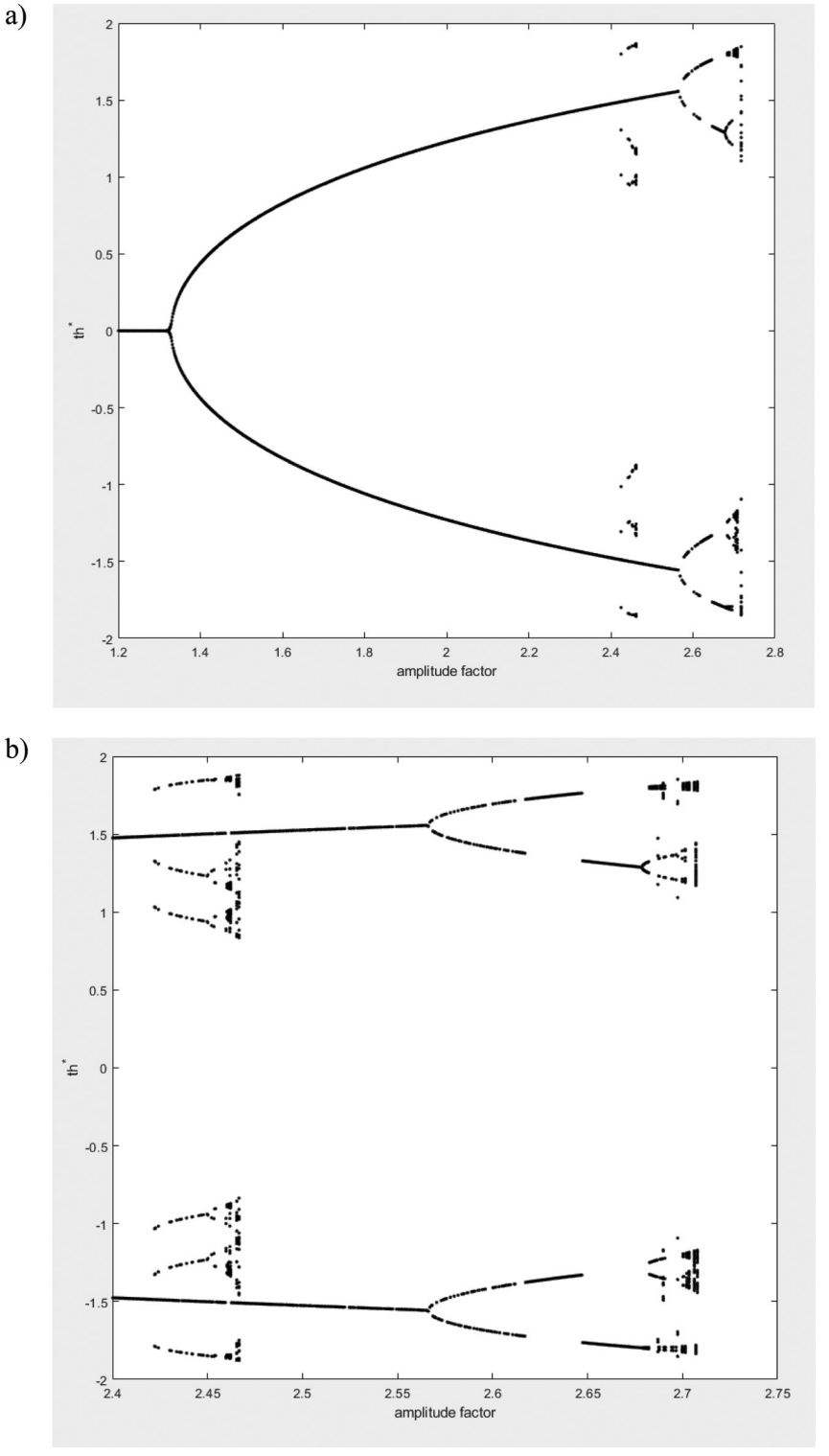

Figure 11. The asymptotic set vs. amplitude factor for $L = 1$ m, $k = 1$ N s and $\omega_0 = 2.5$.

four turning points. Due to the large range of amplitude factor in Figure 11(a), it is not easily discernible but a further period doubling bifurcation occurs at an amplitude factor of 2.7. In Figure 11(b), the asymptotic set is shown for a restricted amplitude factor range,

$$2.4 < \Lambda < 2.8$$

Figure 11(b) shows the period doubling cascade more clearly. The feature identified in Figure 11(a) for the amplitude factor close to 2.4 can be seen to be another period doubling cascade starting with a period of 6. Note the period 6 solution is stable at the same time as the period 2 solution. The trajectory towards either structure is determined by the initial condition, extent of the basin of attractions and small changes in the amplitude factor.

The final figure looking at bifurcation and chaos is Figure 12. In Figure 12, the phase space trajectory once the initial transitory solution is removed from the figure is shown. The pendulum parameters are

$$L = 1m, m = 1\text{kg}, k = 0.5N\,\text{sec}\,\text{and}\,\omega_0 = 2.5$$

with an initial condition of

$$\theta_0 = \frac{\pi}{10}\text{rad}, \dot{\theta}_0 = 0\frac{\text{rad}}{s}$$

The simulation time is 600 s with only the last 60 s of the simulation plotted in phase space. In Figure 12(a), the amplitude factor is $\Lambda = 2.7$. The figure shows a closed cycle of period 8. In Figure 12(b), the simulation is the same as Figure 12(a) except the amplitude factor is increased to $\Lambda = 2.71$. In this case, the phase space trajectory is not a closed cycle, a classic property of a chaotic trajectory.

The sequence of period doubling bifurcations is the classic route to a chaotic system (Sander and Yorke, 2012) where the behaviour of the pendulum becomes extremely erratic and difficult to predict in a quantitative sense. Another property of a chaotic system is the pendulum trajectory is extremely sensitive to the initial conditions of the pendulum, the so-called butterfly effect (Hilborn, 2004) another reason why it is impossible to predict other than in a qualitative sense for large time. Chaotic deterministic systems are more common than you would intuitively believe to be the case. When chaos as a phenomenon was discovered in the 1960s, the search for other chaotic dynamical systems found many deterministic models from many areas of application, from population dynamics in theoretical biology (Figueroa1 et al., 2020) to simple models of fluid motion (Lorenz, 1963) exhibit chaotic behavior.

These linkages with areas outside mechanical engineering are important as it promotes the idea of multidisciplinary teams, and a feeling that mechanical engineers are not an isolated community with their own problems to solve. It promotes an expansive view of the world rather than a narrow perspective. One message from this study is that mechanical engineers have plenty to learn from mathematical biologists!

The study of chaotic dynamic systems is an advanced topic that is part of many mathematical degree programmes but for mechanical engineers this is an area of mathematics that they generally do not come across in their studies. This is an interesting issue as mechanical engineers could well be asked to design a mechanical system that could exhibit chaotic behaviour, by design or not. The closest that an engineer comes to this is the problem of unwanted vibration, but this should not be confused with a chaotic system.

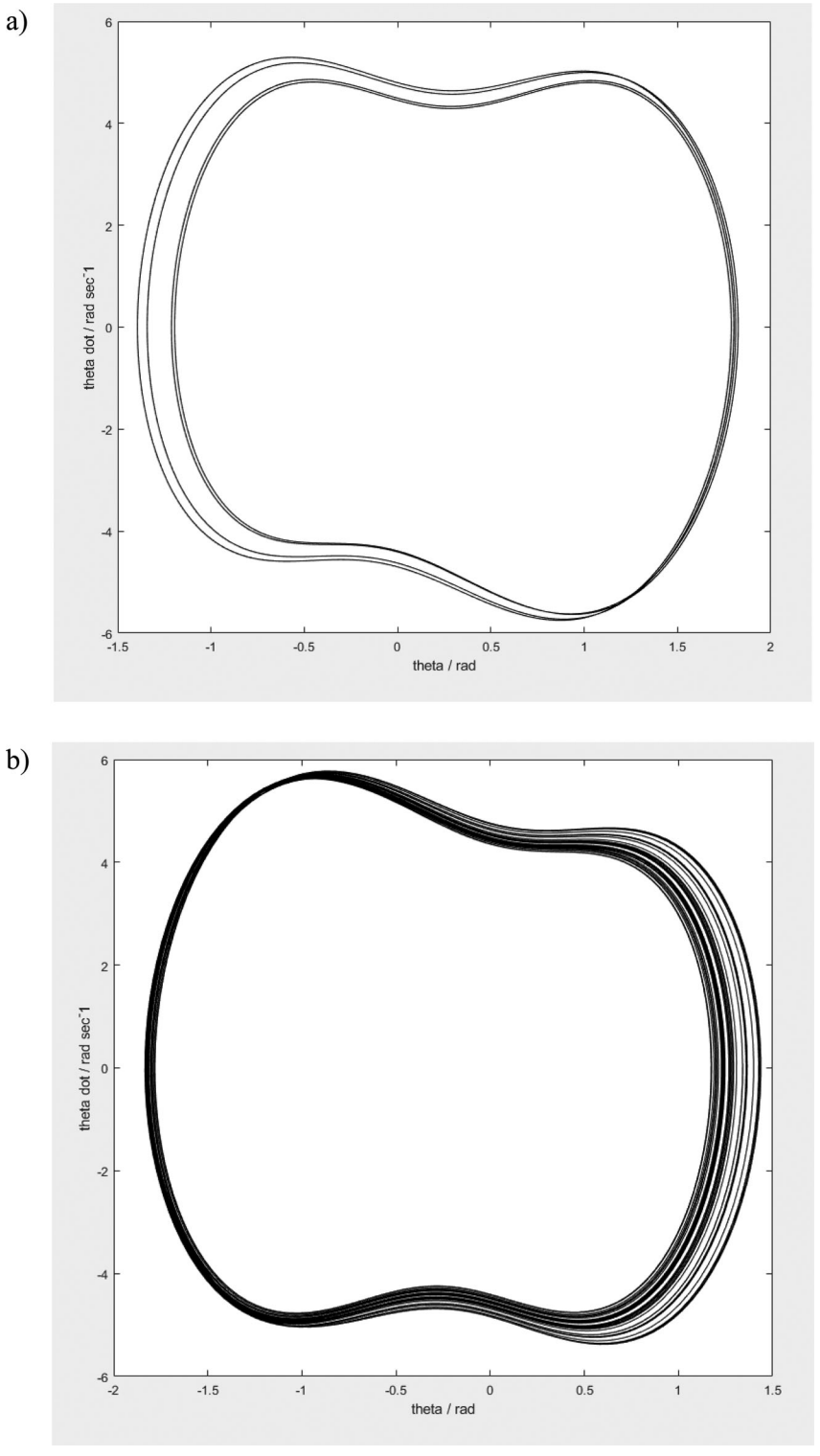

Figure 12. Phase space plots for (a) $(\omega_0, \Lambda, \kappa) = (2.5, 2.7, 0.32)$and (b)$(\omega_0, \Lambda, \kappa) = (2.5, 2.71, 0.32)$.

4. Pendulum models for a child on a swing

In the sections above, we have considered a simple pendulum either forced horizontally or vertically. In the case of a vertically forced pendulum, we have demonstrated a wealth of dynamic behaviour not usually considered by an undergraduate student engineer. Another way to engage a student in the modelling of dynamic systems and dynamic simulation is to consider models of something that a young student engineer will have had first-hand experience of. The simulation of a person on a swing is the example application considered below.

At its essence, a child on a swing can be viewed as a forced pendulum but it can be forced in a number of ways (Bae, 2006; Case 1996). The less adventurous child will sit on the swing and induce motion by changing the location of their centre of mass relative to the horizontal location of the pivot inducing torque about the pivot (Case 1996). A more adventurous, probably older child with little knowledge of health and safety might choose to stand on the swing and again induce torque about the pivot by changing the location of the centre of mass relative to the horizontal location of the pivot. This is labelled as angular forcing in this paper. An alternative approach for the standing child is to, once motion is induced introduce torque into the system by bending their legs for large angular displacements and straightening their legs for small angular displacements (Bae, 2006). In this paper, this strategy is labelled radial forcing.

The possible ways of forcing a swing are shown in Figure 13. To keep things as simple as possible, we will consider the mass of a child on a swing as a point mass and the swing will be connected to the pivot by weightless rods. This is a reasonable approximation for the two standing configurations, Figure 13(a,b). In Figure 13(a) $L(t)$ denotes the distance of the centre of mass of the person on the swing and the pivot. Angular forcing is represented in Figure 13(b,c). In Figure 13(b,c) the angle $\varphi(t)$ represents the angle between the line defined by the centre of mass of the person on the swing and the swing seat and the rods connecting the swing seat to the pivot. For a student sitting on a swing, it is common practice to approximate the body as a point mass, m_1, and the legs as a second point mass, m_2. In Figure 13(c), the distances of m_1 and m_2 from the swing seat are defined to be a_1 and a_2, respectively. In this paper, the system is approximated to be a single-point mass,

$$m = m_1 + m_2 \tag{22}$$

that changes location with respect to the rods connecting the swing seat to the pivot. Labelling the distance of the single centre of mass to the swing seat as L_2, it is possible to show that the single-point mass approximation is accurate only if the following two conditions hold.

$$m_2 \ll m_1 \approx m \tag{23}$$

and

$$a_2 \ll a_1 \approx L_2 \tag{24}$$

see Figure 13(c). This is not particularly interesting as in terms of the proportions of a human body implies that the legs can be neglected in the analysis. This is not an assumption that can be justified in a quantitative analysis. Nevertheless, for the present article it is used

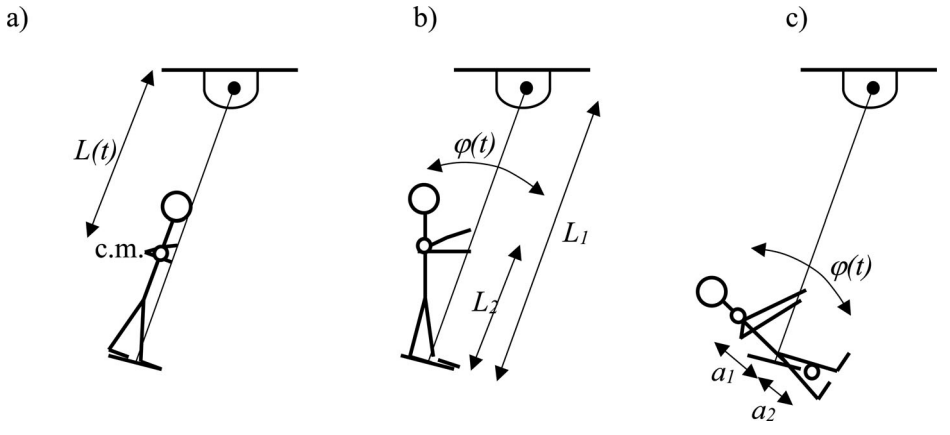

Figure 13. Different approaches to pumping a swing, (a) standing, radial forcing, (b) standing, angular forcing and (c) sitting, angular forcing.

to simplify the equations of motion. It is expected that the qualitative behaviour of the swing dynamics will be similar. The derivation of the model with two masses follows the same approach taken below for the model of an angularly forced pendulum but is more complicated as two-point masses must be considered.

The two different strategies for forcing the swing, involve an angular forcing function and a forcing function that effectively changes the length of the pendulum with time. To fully explore the dynamic behaviour of the two models is not possible in this paper. Attention will be restricted to a derivation of the models and linearizations of models to calculate natural frequencies and demonstrate the simplicity of the linearized models. The angular forcing of a pendulum introduces general curvilinear acceleration and produces a complex model that is probably only grasped by the better student engineers. This is justified in the spirit of providing challenge to the full spectrum of abilities.

4.1. Model for radial forcing

Forcing a swing by bending and extending your legs is equivalent to the length of the pendulum rod changing with time,

$$L(t) = L_0 + A_0 \cos \Omega t \tag{25}$$

This is the functional form for the forcing term given in Bae (2006), where the same model, (28) is derived and analysed. Differentiating (25) with respect to time,

$$\dot{L} = -A_0 \Omega \sin \Omega t$$

$$\ddot{L} = -A_0 \Omega^2 \cos \Omega t$$

This introduces additional accelerations on the pendulum bob associated with general curvilinear coordinates (Meriam and Kraige, 2007).

$$a_t = L\ddot{\theta} + 2\dot{L}\dot{\theta} \tag{26}$$

$$a_n = L\dot{\theta}^2 - \ddot{L}$$

Taking a moment about the pivot and assuming frictional losses are negligible gives the equation of motion

$$-mgL\sin\theta = m\left(L\ddot{\theta} + 2\dot{L}\dot{\theta}\right)L \tag{27}$$

Dividing by mL^2 and rearranging,

$$\ddot{\theta} + 2\frac{\dot{L}}{L}\dot{\theta} + \frac{g}{L}\sin\theta = 0 \tag{28}$$

More details of the model can be found in Bae (2006). To derive the natural frequency of the system, we look at the small angle approximation and assume the forcing amplitude, A_0 is small relative to the unforced pendulum length, L_0.

$$\ddot{\theta} + \frac{g}{L_0}\theta = 0 \tag{29}$$

Giving a natural frequency of

$$\omega = \sqrt{\frac{g}{L_0}} \tag{30}$$

4.2. Numerical simulation of a radially forced pendulum

When considering the pendulum equation as a model for a swing being forced by bending and straightening the legs, the following parameters would represent values appropriate for a young adult,

$$L_0 = 1.8m, A_0 = 0.2m, \omega = 2.33\frac{1}{s}$$

With a swing length of 3 m, this is equivalent to the persons centre of mass being 1.2 m above the swing seat. To initiate motion of the swing the initial condition cannot be the steady state, $\theta = 0$. Therefore, the initial condition is the equivalent of a friend introducing an impulse to the swing to initiate motion.

$$(\theta_0, \dot{\theta}_0) = (0, 1)$$

A numerical simulation for the model with the parameters given above is shown in Figure 14. Note there are three curves shown in the figure representing three different forcing frequencies. For the full line simulation, the forcing frequency is half the natural frequency, $\Omega = 1.17$ 1/s. For this forcing condition, the amplitude of the swing is approximately 0.5 radians. Increasing the forcing frequency to $\Omega = 2.33$ 1/s, the dotted line in Figure 14, does not change the swing trajectory significantly. In the final simulation, the dashed line in Figure 14 the forcing frequency is increased to double the natural frequency, $\Omega = 4.67$ 1/s. For this forcing condition, the maximum amplitude is 1.7 radians. The swing trajectory is qualitatively different from the other two simulations, in that there is a high–frequency motion with a low-frequency component superimposed on it. The maximum amplitude occurring for a forcing frequency that is double the natural frequency is consistent with results in the literature (Glendinning, 2020) and can be understood using a

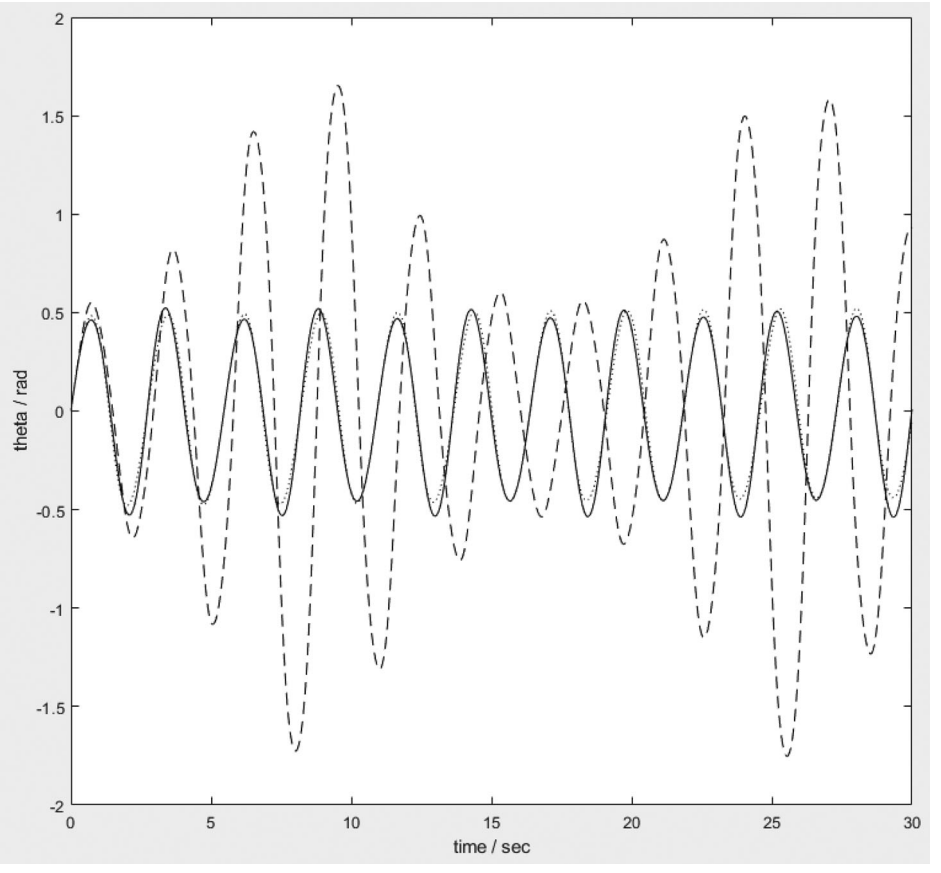

Figure 14. Angular displacement vs. time, radial forcing, $L_0 = 1.8m, A_0 = 0.2m$, full line – $\Omega = 1.17$ 1/s, dotted line – $\Omega = 2.33$ 1/s, and dashed line – $\Omega = 4.67$ 1/s.

geometric argument. Anyone that has played on a swing knows that normal swing dynamics cannot be described as a high-frequency oscillation of the swing with the maximum amplitude varying with time as shown in Figure 14. The reason for this is that we are modelling the swings forcing term as if it is powered by an electric motor or some other device. The reality is that a person does not force the swing in this way they use a technique called adaptive resonance (Glendinning, 2020). Adaptive resonance means that the forcing of the swing by a person follows a strategy such that the distance between the centre of mass and the pivot is minimized at $\theta = 0$ and maximized where the angular velocity, $\dot{\theta}$ is zero. This implies that a forcing term depending on angular displacement rather than time would potentially yield a more realistic pendulum trajectory.

4.3. Model for angular forcing

The model for forcing a swing by moving the centre of mass from side-to-side, changing the angular displacement, pivoting about the waist if sitting down or pivoting at the feet if standing up is more complicated than the models we have discussed above. Figure 15 shows

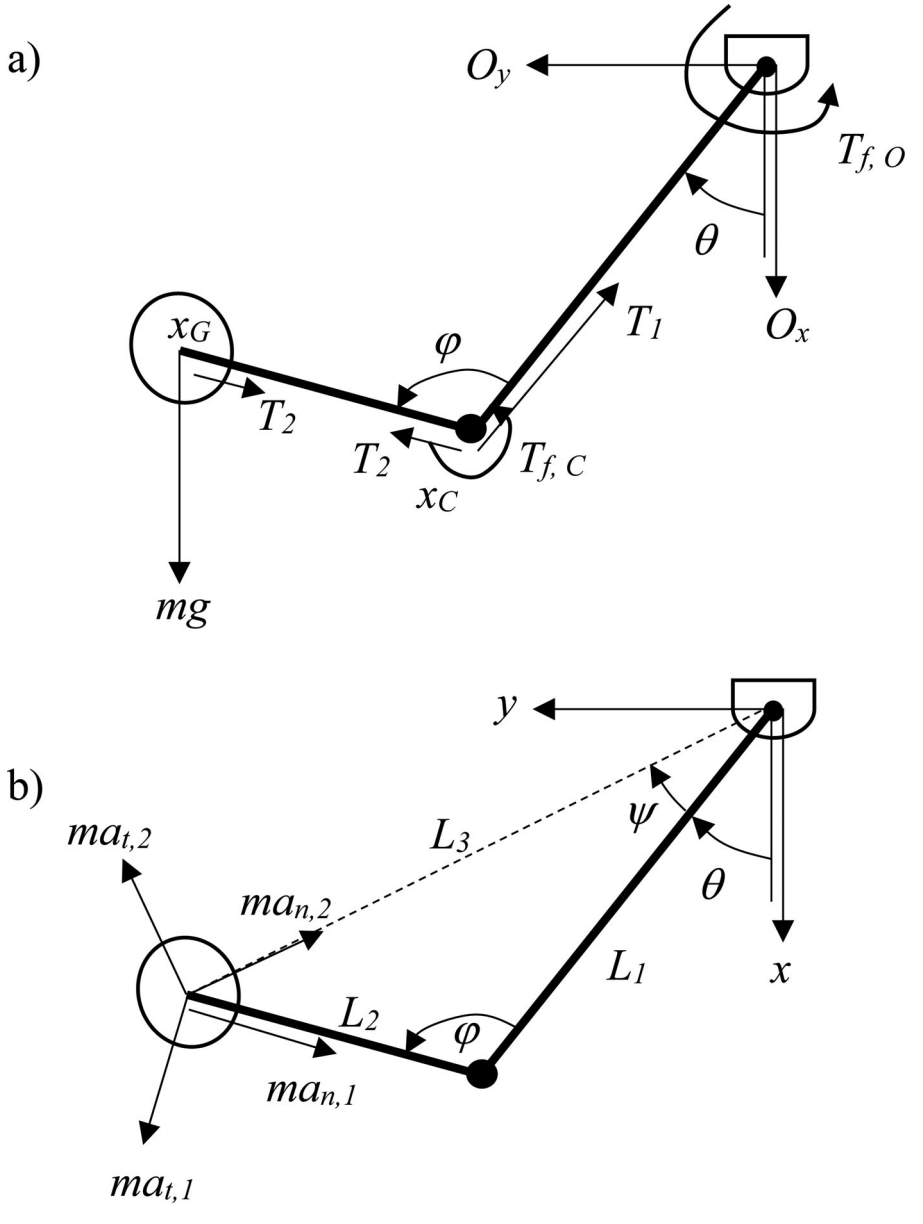

Figure 15. Free body diagram and mass acceleration diagram for a model of a swing with angular forcing.

the free body diagram and mass acceleration diagram for the system. Similar to the leg bending model we will neglect friction in the derivation and the body will be represented as a point mass.

The motion of the centre of mass is given the functional form,

$$\varphi(t) = \varphi_0 \cos \Omega t \tag{31}$$

This is the same forcing function used in Case (1996). The derivatives of the forcing function, (31) are then,

$$\dot{\varphi} = -\varphi_0 \Omega \sin \Omega t$$
$$\ddot{\varphi} = -\varphi_0 \Omega^2 \cos \Omega t$$

One complication of forcing the pendulum in this way is there are a number of mass accelerations in the mass acceleration diagram shown in Figure 15(b). The mass is being accelerated from side to side about the pivot located at x_C, see Figure 15(b), and at the same time is undergoing an acceleration about the pivot located at O. In Figure 15 all point vectors are relative to the pivot, O, x_G denotes the location of the pendulum bob and x_C denotes the location that the two connecting rods join. The internal force, T_2 in Figure 15, represents the internal tension within the connecting rod between x_C and x_G. This acts within the rod at both ends and in terms of the motion of the pendulum has no influence as they cancel each other in the moment equation (37) derived below. Considering the mass acceleration diagram, Figure 15(b), this is curvilinear motion, and the accelerations take the form,

$$a_{t,1} = L_2 \ddot{\varphi} \tag{32}$$
$$a_{n,1} = L_2 \dot{\varphi}^2 \tag{33}$$
$$a_{t,2} = L_3 \left(\ddot{\theta} + \ddot{\psi}\right) + 2\dot{L}_3(\dot{\theta} + \dot{\psi}) \tag{34}$$
$$a_{n,2} = L_3(\dot{\theta} + \dot{\psi})^2 - \ddot{L}_3 \tag{35}$$

The two accelerations, (32) and (33) represent the tangential acceleration and centripetal acceleration associated with the rotation about the point x_C,see Figure 15. L_2 denotes the magnitude of the vector, x_G-x_C. The two accelerations, (34) and (35) represent the accelerations in the tangential direction with respect to the vector x_G and the acceleration in the normal direction at x_G directed back towards O. Note the length of x_G, labelled L_3 in Figure 15 is changing with time. This means that the first and second derivatives of L_3 must be included in the accelerations, (34) and (35) (Meriam and Kraige, 2007).

Taking a moment about, O to give the equations of motion is a much more complicated process than the other models in this paper as the lines of action for the forces and mass accelerations relative to the pivot, O can be difficult to calculate. Another approach is required. To this end, some of the moments are represented using the cross-product operation between the point vector and the mass acceleration (Meriam and Kraige, 2007).

$$dma = m(x \times a) \tag{36}$$

Where d is the perpendicular distance between the line of action of the acceleration, a and the pivot O, and x is the point vector. As already stated, this is a significantly more complicated forced pendulum to derive the equations of motion for and it would be unrealistic to expect even the most talented student engineers on an introductory dynamics course to have the capability to derive the model. It is included here to show what is possible when applying these mathematical constructs to dynamic systems. It should be viewed as a partial vision of the material presented in more advanced courses in dynamics. The equation

of motion derived by taking a moment about O is as follows:

$$-mg(L_1 \sin\theta + L_2 \sin(\varphi - \theta)) - T_{f,O} - T_{f,C} = \\ ma_{t,2}L_3 - ma_{t,1}X_{t,1}|x_G \times t_1| - ma_{n,1}X_{n,1}|x_G \times n_1| \tag{37}$$

The frictional loss at the pivot and the joint connecting the two rods are denoted by $T_{f,O}$ and $T_{f,C}$, respectively. Note there are four mass acceleration terms in Figure 15, yet only three are found in (37). The reason for this is the line of action for $a_{n,2}$ passes through the pivot so makes no contribution. Some of the other terms in (37), require further explanation, $X_{t,1}$ and $X_{t,2}$ are terms introduced to take account of the sense of rotation of the moments and are defined below. The unit vectors, t_1 and n_1 are defined to have directions to be the tangential direction and normal direction, respectively, see Figure 15,

$$n_1 = -\frac{x_G - x_C}{|x_G - x_C|} \tag{38}$$

$$t_1 = \begin{pmatrix} -n_{1,y} \\ n_{1,x} \end{pmatrix} \tag{39}$$

$X_{t,1}$ and $X_{n,1}$ are given below. The logic for $X_{t,1}$ will be presented, the formulation for $X_{n,1}$ is the same. The equation of a line passing through x_G in the direction t_1 and parameterized by λ is,

$$\begin{pmatrix} x_\lambda \\ y_\lambda \end{pmatrix} = x_G + \lambda t_1 \tag{40}$$

The value of λ for the line to cross the y-axis is

$$\lambda^* = -\frac{x_{G,x}}{t_{1,x}} \tag{41}$$

This is assuming that t_1 is not parallel to the y-axis. If it is parallel to the y-axis, then deciding the sense of rotation of the moment is straight forward. In either case, we have a criterion for determining $X_{t,1}$ to indicate the sense of rotation of the moment.

$$X_{t,1} = \begin{Bmatrix} 1 & y_{\lambda^*} > 0 \text{ or } t_1 = -j \\ 0 & y_{\lambda^*} = 0 \\ -1 & y_{\lambda^*} < 0 \text{ or } t_1 = j \end{Bmatrix} \tag{42}$$

Where j represents the unit vector in the direction of the y-axis.

Assuming the frictional losses are small and can be ignored and substituting for the tangential and normal accelerations in (37), dividing by the mass and rearranging such that terms involving θ, and its derivatives are on the left-hand side and all-time dependent terms on the right gives

$$L_3^2\ddot{\theta} + 2L_3\dot{L}_3\dot{\theta} + gX_g(L_1 \sin\theta + L_2 \sin(\varphi - \theta)) = \\ -L_3^2\ddot{\psi} - 2L_3\dot{L}_3\dot{\psi} + X_{t,1}|x_G \times t_1|L_2\ddot{\varphi} + X_{n,1}|x_G \times n_1|L_2\dot{\varphi}^2 \tag{43}$$

The terms, L_3 and ψ and their derivatives require further work to express in terms of known parameters. Considering Figure 15, applying the cosine rule to the triangle gives an

expression for L_3.

$$L_3^2 = L_1^2 + L_2^2 - 2L_1L_2\cos\varphi \tag{44}$$

This can be differentiated twice to give,

$$L_3\dot{L}_3 = L_1L_2\sin\varphi\dot{\varphi}$$
$$L_3\ddot{L}_3 + \dot{L}_3^2 = L_1L_2\left(\cos\varphi\dot{\varphi}^2 + \sin\varphi\ddot{\varphi}\right)$$

Similarly applying the sine rule gives the following equation:

$$L_3\sin\psi = L_2\sin\varphi \tag{45}$$

Which can then be differentiated twice,

$$\dot{L}_3\sin\psi + L_3\cos\psi\dot{\psi} = L_2\cos\varphi\dot{\varphi}$$
$$\ddot{L}_3\sin\psi + 2\dot{L}_3\cos\psi\dot{\psi} - L_3\sin\psi\dot{\psi}^2 + L_3\cos\psi\ddot{\psi} = L_2\left(-\sin\varphi\dot{\varphi}^2 + \cos\varphi\ddot{\varphi}\right)$$

Given initial conditions we now have a closed system a second-order differential equation (43) and associated equations (44) and (45).

This is a complicated system, but as far as numerical simulation is concerned does not represent that much more of a challenge to solve in MATLAB than the other pendulum models.

When evaluating the natural frequency of the system, consider a system where the angular displacements, θ and φ are small then the expression for the length, L_3 simplifies to a constant,

$$L_3 = L_1 - L_2 \tag{46}$$

Returning to the application of the sine rule, (45), then provided L_3 is not small relative to L_2

$$\begin{aligned}\psi &= \frac{L_2}{L_1 - L_2}\varphi \\ \dot{\psi} &= \frac{L_2}{L_1 - L_2}\dot{\varphi} \\ \ddot{\psi} &= \frac{L_2}{L_1 - L_2}\ddot{\varphi}\end{aligned} \tag{47}$$

The second-order differential equation, (43), is reduced to,

$$(L_1 - L_2)^2\ddot{\theta} + g(L_1 - L_2)\theta = -gL_2\varphi \tag{48}$$

This gives a natural frequency,

$$\omega = \sqrt{\frac{g}{L_1 - L_2}} \tag{49}$$

and the equation of motion becomes,

$$\ddot{\theta} + \omega^2\theta = -g\left(\frac{L_2}{L_1 - L_2}\right)\varphi_0\cos\Omega t \tag{50}$$

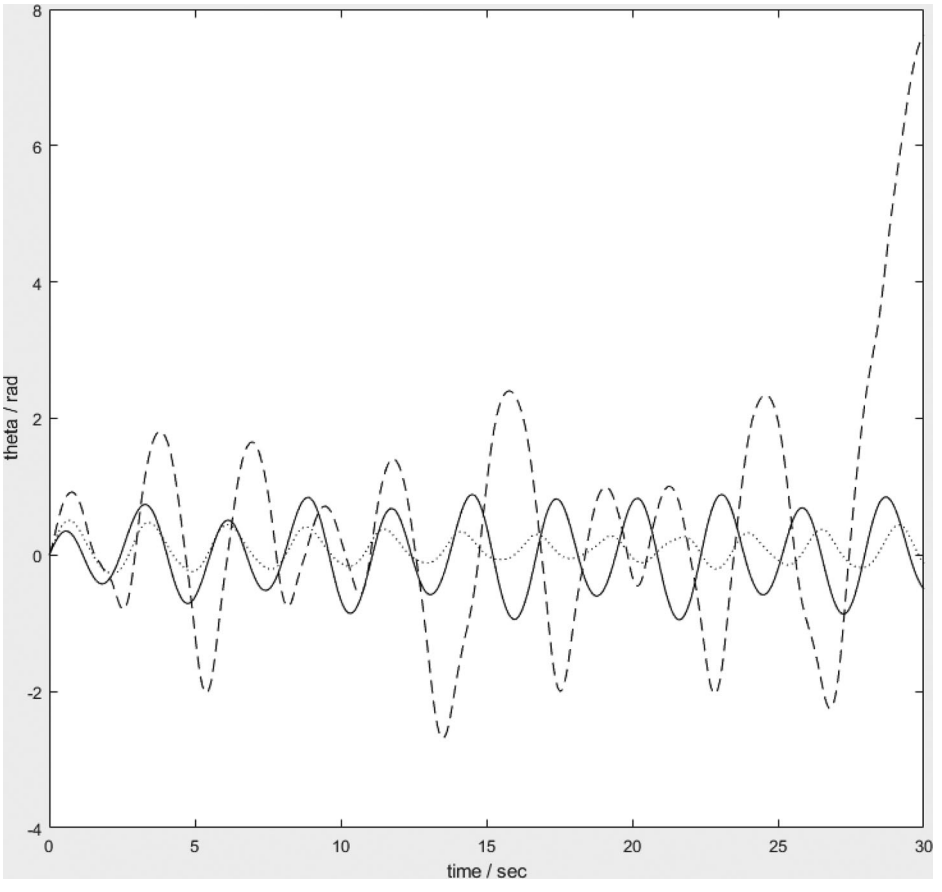

Figure 16. Angular displacement vs. time, angular forcing while standing, $L_0 = 1.8m, \varphi_0 = 0.3\text{rad}$, full line – $\Omega = 1.17$ 1/s, dotted line – $\Omega = 2.33$ 1/s, and dashed line – $\Omega = 4.67$ 1/s.

4.4. Numerical simulations of an angularly forced pendulum

We can now solve (43) for a set of swing conditions to represent swing motion for a person standing up and moving the swing with angular forcing,

$$L_0 = 1.8m, \varphi_0 = 0.3\text{rad}, \omega = 2.33\frac{1}{s}$$

L_0 remains the same as the leg bending approach as the person is still standing on the swing. The maximum angular displacement of the forcing term, φ_0, is derived from assuming an arm length of 0.5 m and the centre of mass is 1.2 m above the swing seat. Figure 16 shows the angular displacement for the three forcing conditions differentiated by the forcing frequency for standing angular forcing of the swing. Note the maximum amplitude changes with time when the pendulum is forced with angular forcing. Another difference to the leg bending approach is the maximum angular displacement is less with a forcing frequency of 2.33 1/s compared to a forcing frequency of 1.17 1/s. The final point of note is the maximum angular displacement for a forcing frequency of 4.67 1/s is growing with time and reaches a point where rotational motion of the swing is induced at approximately $t = 27$ s. When on

a swing, inducing rotational motion is a very rare event, if not impossible. Therefore, it is very unlikely that the model's prediction is correct. There are two possible reasons for why rotational motion is predicted but, unlikely. No energy dissipation due to frictional losses is included in the model is one reason and the second is that it is unlikely that a person can force the swing at a frequency of 4.67 1/s.

In Figure 17, the simulation of a person in a seated position, modelled as a single-point mass is shown. For this simulation, the pendulum parameters are specified as,

$$L_0 = 2.4m, \varphi_0 = 0.6\text{rad}, \omega = 2.02\frac{1}{s}$$

These values are justified on the basis of halving the distance from the swing seat to the centre of mass and doubling the maximum angle for the forcing term. Given the deficiencies of the model relative to a two-mass model it does not seem justified to do a deep analysis of what the pendulum characteristics should be for a person sitting on the swing and applying angular forcing. For this configuration, the natural frequency is reduced as the distance from the pivot to the centre of mass increases. Figure 17 shows the angular displacement vs. time for the three different forcing frequencies, $\Omega = 1.01, 2.02$ and 4.04 1/s. The results have similarities and differences to both of the other two simulations. Similar to the radial forcing simulation the angular displacement is oscillating for all three forcing frequencies. The likelihood of rotational motion is reduced when comparing angular forcing from a sitting position compared to a standing position as halving the distance of the centre of mass from the swing seat, (L_2) and doubling the angular range of the forcing term, (φ_0) overall reduces the addition of rotational kinetic energy introduced to the system as the mass moment of inertia for the point mass depends on the square of the length and linearly depends on the angular range of the forcing term. Another interesting difference between Figures 16 and 17 is the maximum angular displacement for the three forcing frequencies, $\omega_0 = 0.5$, 1 and 2 are in a different order. In Figure 16, the simulation with $\omega_0 = 0.5$ the simulation has a bigger maximum angular displacement than $\omega_0 = 1$. In Figure 17, the reverse is the case. This has been checked several times and the behaviour is rigorous. As yet the author does not have an explanation for this, and further investigation is required. The discussion of the dynamics of a swing in this section is the first stages of an exploration of the model's behaviour and there are many questions to answer. Another important message for undergraduate student engineers is research is analogous to the growth of a tree with research often asking more questions than answering questions.

5. Conclusion

In this paper, it has been demonstrated that there is so much more to pendulum dynamics than is generally presented to the undergraduate mechanical engineering population. We have pendulums that exhibit stable states that become unstable when forced in a particular way and unstable states that become stable when forced in a particular way.

This behaviour has been further explored to show that the set of conditions that tend to a vertical upright orientation, the basin of attraction, is an interesting set with a beautiful structure that depends on the degree of energy dissipation due to frictional losses. The basin of attraction analysis has been further extended to gain insight into the stability

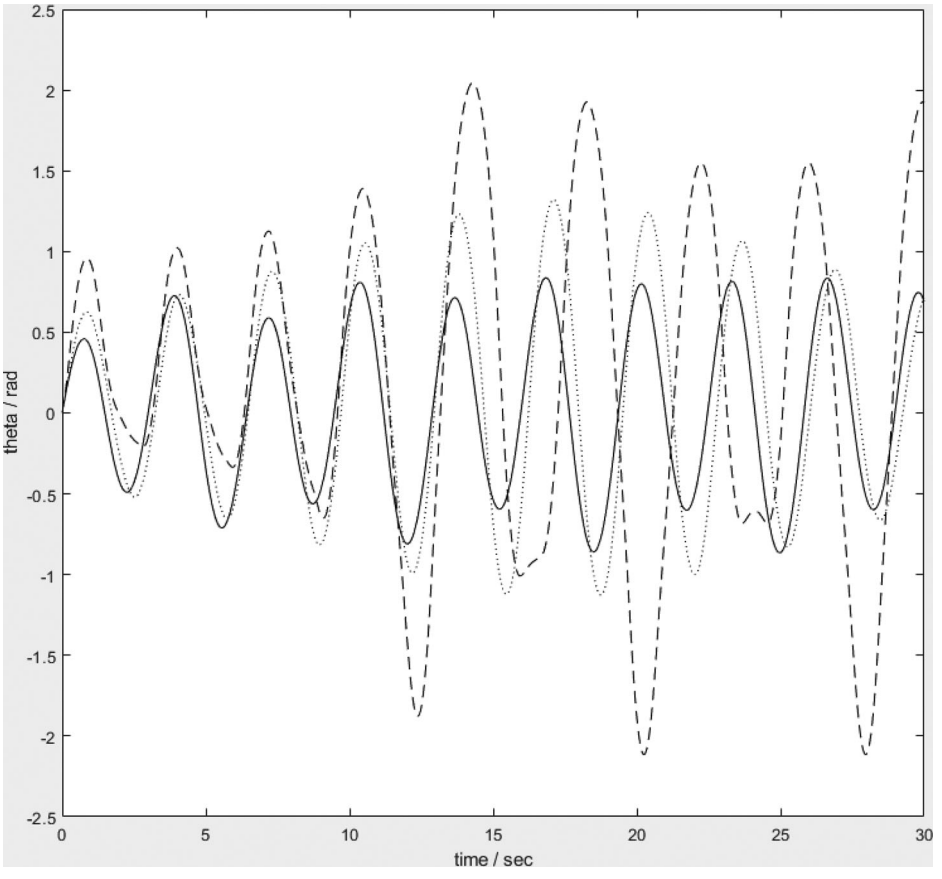

Figure 17. Angular displacement vs. time, angular forcing while sitting, $L_0 = 2.4m, \varphi_0 = 0.6$rad, full line – $\Omega = 1.01$ 1/s, dotted line – $\Omega = 2.02$ 1/s, and dashed line – $\Omega = 4.04$ 1/s.

region in frequency factor/amplitude factor space. The structure of these regions is complex and leads onto the interesting question of in regions of instability of the steady states 'What happens in these regions of parameter space?'

Using techniques from dynamical system analysis, notably Poincare maps and a focus on the asymptotic behaviour of the forced pendulum it is clear that a rich behaviour for the pendulum dynamic behaviour exists. For a given value of the frequency factor as the amplitude factor is systematically increased stationary points change stability, either being stable and then becoming unstable or vice versa. Following the stable condition as the amplitude factor increases further the stationary point loses stability leading to a sequence of successive period doubling bifurcations changing the stationary point to an oscillating solution. Following the first bifurcation, the stationary point changes to an oscillating solution, oscillating between two angular displacements. The next bifurcation changes the solution to one that oscillates through four maximum angular displacements. Following the sequence of period doubling bifurcations the pendulums trajectory is one that follows a chaotic path. In this context, a chaotic trajectory is one where the pendulums motion is erratic and is sensitive to the initial conditions.

All of the above would spark even the least motivated mechanical engineering students interests in what most people would consider a mundane dynamic system.

Further to promoting interest an application of pendulums to something that all students would have experience of, a child playing on a swing. The model is presented, and a limited investigation of pendulum behaviour is given. On purpose these dynamic systems promote many questions that an interested student could identify and propose paths forward to investigate further.

Conflict of interest

The author can confirm that there is no conflict of interest relating to this paper.

Disclosure statement

No potential conflict of interest was reported by the author.

References

Andreeva, T., Alevras, P., Naess, A., & Yurchenko, D. (2016). Dynamics of a parametric rotating pendulum under a realistic wave profile. *International Journal of Dynamics and Control*, *4*(2), 233–238. https://doi.org/10.1007/s40435-015-0168-z

Bae, S. (2006). Equivalence of the pumping of a swing and the pumping of a swing and the parametric resonance. *European Journal of Physics*, *27*(2), 291–298. https://doi.org/10.1088/0143-0807/27/2/012

Belendez, A., Hernandez, A., Marquez, A., Belendez, T., & Neipp, C. (2006). Analytical approximations for the period of a nonlinear pendulum. *European Journal of Physics*, *27*(3), 539–551. https://doi.org/10.1088/0143-0807/27/3/008

Berry, J. S., Savage, M., & Williams, J. (1989). Mechanics in decline? *International Journal of Mathematical Education in Science and Technology*, *20*(2), 289–296. https://doi.org/10.1080/0020739890200209

Big-Alabo, A. (2020). Approximate periodic solution for the large amplitude oscillations of a simple pendulum. *International Journal of Mechanical Engineering Education*, *48*(4), 335–350. https://doi.org/10.1177/0306419019842298

Biggoggero, G. F., & Rovida, E. (1977). Problems in the teaching of mechanics. *European Journal of Engineering Education*, *2*(4), 277–290. https://doi.org/10.1080/0304379770020406

Butikov, E. (2001). On the dynamic stabilization of an inverted pendulum. *American Journal of Physics*, *69*(7), 755–768. https://doi.org/10.1119/1.1365403

Case, W. B. (1996). The pumping of a swing from a standing position. *American Journal of Physics*, *64*(3), 215–220. https://doi.org/10.1119/1.18209

Cumber, P. S. (2015). Waggling pendulums and visualisation in mechanics. *International Journal of Mathematical Education in Science and Technology*, *46*(4), 611–630. https://doi.org/10.1080/0020739X.2014.987838

Cumber, P. S. (2016). Waggling conical pendulums and visualisation in mechanics. *International Journal of Mathematical Education in Science and Technology*, *47*(4), 612–636. https://doi.org/10.1080/0020739X.2015.1088085

Cumber, P. S. (2017). Visualisation in mechanics: The dynamics of an unbalanced roller. *International Journal of Mathematical Education in Science and Technology*, *48*(3), 434–454. https://doi.org/10.1080/0020739X.2016.1248509

Cumber, P. S. (2021). Visualising mechanics: Washing machine dynamics. *International Journal of Mathematical Education in Science and Technology*, *52*(4), 626–652. https://doi.org/10.1080/0020739X.2020.1794070

Fay, T. H. (2002). The pendulum equation. *International Journal of Mathematical Education in Science and Technology*, *33*(4), 505–519. https://doi.org/10.1080/00207390210130868

Figueroa1, W., Prada1, D., Vera, P., Gomez, J., Montes, E., & Bautista, G. (2020). Analysis of population dynamics and chaos theory. *Journal of Physics: Conference Series*, *1448*(1), 012001. https://doi.org/10.1088/1742-6596/1448/1/012001

Glendinning, P. (2020). Adaptive resonance and pumping a swing. *European Journal of Physics*, *41*(2), 025006. https://doi.org/10.1088/1361-6404/ab6a63

Glyn, J., & Dyke, P. (2020). *Modern engineering mathematics, 6th Edn*. Pearson.

Graham, E., & Peek, A. (1997). Developing an approach to the introduction of rigid body dynamics. *International Journal of Mathematical Education in Science and Technology*, *28*(3), 373–380. https://doi.org/10.1080/0020739970280307

Graham, E., & Rowlands, S. (2000). Using computer software in the teaching of mechanics. *International Journal of Mathematical Education in Science and Technology*, *31*(4), 479–493. https://doi.org/10.1080/002073900412598

Guckenheimer, J., & Holmes, P. J. (2002). *Nonlinear oscillations, dynamical systems, and bifurcations of vector fields*, 6th Edition. Springer.

Hilborn, R. C. (2004). Seagulls, butterflies and grasshoppers: A brief history of the butterfly effect in nonlinear dynamics. *American Journal of Physics*, *72*(4), 425–427. https://doi.org/10.1119/1.1636492

Kapitza, P. L. (1965). Dynamic stability of the pendulum with vibrating suspension point, 1951. In D. Ter Haar (Ed.), *Collected papers of P.L. Kapitza* Vol. 2, (pp. 714–726). London: Pergamon.

Knight, D. G. (2004). Classroom note: Maple® version of the 'Indian rope trick'. *International Journal of Mathematical Education in Science and Technology*, *35*(1), 126–134. https://doi.org/10.1080/00207390310001623490

Lambert, J. D. (1991). *Numerical methods for ordinary differential systems: The initial value problem*. John Wiley.

Lorenz, E. N. (1963). Deterministic nonperiodic flow. *Journal of the Atmospheric Sciences*, *20*(2), 130–141. https://doi.org/10.1175/1520-0469(1963)020 < 0130:DNF > 2.0.CO;2

Meriam, J. L., & Kraige, L. G. (2007). *Engineering mechanics dynamics 6th Edn*. John Wiley.

Nayfeh, A. H. (1993). *Introduction to perturbation techniques*. John Wiley and Sons.

Sander, E., & Yorke, J. A. (2012). Connecting period-doubling cascades to chaos. *International Journal of Bifurcation and Chaos*, *22*(2), 1250022. https://doi.org/10.1142/S0218127412500228

Stephenson, A. (1908). On a new type of dynamic stability. *Mem Proc. Manch Lit Phil. Soc*, *52*(8), 1–10.

Wright, J. A., Bartuccelli, G., & Gentile, M. G. (2014). The effects of time-dependent dissipation on the basins of attraction for the pendulum with oscillating support. *Nonlinear Dynamics*, *77*(4), 1377–1409. https://doi.org/10.1007/s11071-014-1386-1

Yurchenko, D., & Aleras, P. (2013). Dynamics of the N-pendulum and its application to a wave energy converter concept. *International Journal of Dynamics and Control*, *1*(4), 290–299. https://doi.org/10.1007/s40435-013-0033-x